**Title**

Specificity of Solvatochromic Trehalose Probes for Mycobacteria Detection



**Author**

Kumar, Shivani Shalini

**Publication Date**

2024

Peer reviewed|Thesis/dissertation

UNIVERSITY OF CALIFORNIA

Los Angeles

# Specificity of Solvatochromic Trehalose Probes for Mycobacteria Detection

A thesis submitted in partial satisfaction

of the requirements for the degree

Master of Science in Bioengineering

by

Shivani Shalini Kumar

2024

ABSTRACT OF THE THESIS

Specificity of Solvatochromic Trehalose Probes for Mycobacteria Detection

by

Shivani Shalini Kumar

Master of Science in Bioengineering

University of California, Los Angeles, 2024

Professor Mireille Kamariza, Chair

Tuberculosis (TB) remains as the second leading infectious killer worldwide. In 2022 alone, 1.3 million people died from TB, with the disease being most prevalent in low-resource countries. In these settings with high TB prevalence, access to expensive diagnostic tools is limited, making the development of fast, sensitive, specific and low-cost diagnostic methods crucial. Here, we employ the 4-*N,N*-dimethylamino-1,8-naphthalimide–conjugated trehalose (DMN-Tre) and 3-Hydroxychromone-conjugated trehalose (3HC-Tre) solvatochromic trehalose conjugated fluorogenic dyes to probe the unique properties of mycobacteria and other *Actinomycetales*. These conjugates are incorporated into the mycomembrane as trehalose dimycolates, where they fluoresce upon contact with the hydrophobic environment of the mycomembrane. For these probes to facilitate faster diagnostics, they must specifically target mycobacteria, eliminating the requirement of extensive pre-processing of clinical samples. This thesis presents the results of specificity testing for both DMN-Tre and 3HC-Tre. Using flow cytometry, plate reader and microscopy, this research demonstrates that DMN-Tre exhibits specificity for mycobacteria. In contrast, 3HC-Tre demonstrated limited specificity. These findings suggest that DMN-Tre has the potential to be developed into a rapid, low-cost diagnostic tool for TB, tailored to the needs of resource-limited settings.

The thesis of Shivani Shalini Kumar is approved.

Dino Di Carlo

Aaron S. Meyer

Mireille Kamariza, Committee Chair

University of California, Los Angeles

2024

**Acknowledgements**

Thank you, Dr. Mireille Kamariza, for your continuous support, encouragement, and guidance. Thanks to your mentorship I have grown tremendously as a scientist and engineer. Your passion and dedication to uplifting communities in need and being a voice for the underserved is truly inspiring. I will carry this dedication to underprivileged communities with me as a guiding principle throughout my career as a bioengineer.

Thank you to Lilith Schwartz and Austin Si for helping me grow as a scientist, supporting me throughout my thesis and being such wonderful friends. Thank you to Ashley Clemens for helping me with the microscopy portion of my thesis. I appreciate your patience and support.

Thank you so much to everyone in the Kamariza lab for creating a collaborative, supportive environment. Over the past year, I have learned so much and made lifelong friends. I am grateful for the opportunity to have joined the Kamariza lab in its first few months at UCLA and watch the lab grow and flourish. This lab is so special: an uplifting community of scientists who lift each other up. I am so excited to see all the wonderful things you all accomplish!

**Dedication**

Thank you to my parents, Shalini and Kiran. I am eternally grateful for your continued support and for prioritizing my mental and physical health. Your deep love and care for others have profoundly shaped me in countless ways. Thank you to my brother, Om, for your friendship and support. I am so grateful to have a sibling whom I can truly call my best friend. To my grandmother, Uma, thank you for your unwavering support and pure love. I cherish every moment we have spent together, and I am extremely grateful for your positive and joyful presence in my life. To my late grandfather, Dr. Nagendrappa, your passion and commitment to providing medical care for those in need has always inspired me. Thank you for teaching me what it means to be an upstanding citizen and devoted family member.

## TABLE OF CONTENTS

## Chapter 1: Introduction

Tuberculosis (TB) remains an urgent global health issue, ranking as the second leading cause of death worldwide, following closely behind the coronavirus disease.[1] According to the World Health Organization (WHO), a staggering 10.6 million people fell sick with TB and 1.30 million people died from TB in 2022 alone.[1] 87% of TB cases are concentrated in 30 countries with high TB burden, including India, Indonesia, China, the Philippines and Pakistan.[1] There is a clear disparity in TB incidence worldwide, with the majority of cases being consolidated to 15% of countries. This data highlights the findings that countries with lower GDP per capita tend to have higher rates of *Mycobacterium tuberculosis* (Mtb) infection.[1] Additionally, there is a positive correlation between the prevalence of undernourishment and the incidence of TB, indicating that malnutrition and poverty are key attributors of the disease.[1]

To effectively alleviate the TB burden in these countries, it is crucial to focus on the specific needs of these regions. Providing diagnostic and therapeutic care that is relevant and useful for low-resource settings is essential. **By addressing these challenges with cost-effective and low-resource-friendly solutions, we can make significant strides in reducing the global TB burden and improving health outcomes in the most affected areas.**

Currently, the three main diagnostic tools for Mtb are sputum smear microscopy, mycobacterial culture and nucleic acid amplification tests.[2] The Ziehl-Neelsen (ZN) smear microscopy test focuses on the acid-fast characteristics of mycobacteria.[2] The test is simple, inexpensive and specific to the acid-fast properties of *Mycobacterium* and *Nocardia*.[2] However, the test only has a 50% true-positive rate for those with active cases of TB.[2] Mycobacterial culture is another

commonly used diagnostic and has been shown to be more sensitive than the Ziehl-Neelsen smear.[2] The main limitation of this diagnostic tool is that it requires weeks to complete. Mtb has a doubling time of 24-30 hours.[2] This slow replication rate means that culture tests can take 4-6 weeks to become positive on solid media and 10-21 days in liquid media.[2] This time period can be the difference between positive or negative health outcomes for patients who are in need of immediate care. Nucleic acid amplification tests, specifically the GeneXpert (MTB/RIF) have shown promising results.[2] The GeneXpert is able to report on Mtb and rifampicin (RIF) resistant Mtb.[2] It provides rapid results with high sensitivity and specificity.[2] However, there are some drawbacks including the price, stringent maintenance protocols and involved and specialized instrumentation.[3] Previously, international donations have enabled the establishment of GeneXperts in low-resource settings.[3] But these donations are not constant which can lead to difficulty in implementation.[3]

Drug resistant Mtb is a significant global health challenge. Antibiotic resistance to at least isoniazid and rifampicin (two first-line drugs) is defined as multidrug-resistant tuberculosis (MDR TB).[1] Extensively drug-resistant resistant tuberculosis (XDR TB) is defined as resistance to second-line drugs and can cause even further complications in treatment outcomes.[1] In 2022 alone, 410,000 people were diagnosed with MDR TB, but unfortunately only 40% of those people were diagnosed and received treatment.[1] A major issue is the lack of appropriate diagnosis and therapeutic care provided for people with MDR TB. Ten countries account for 70% of people who have MDR TB and have not received the appropriate diagnostic and therapeutic care required.[1] Addressing the needs of these countries with high MDR TB burden and creating diagnostic and therapeutic

solutions that are relevant and meet their specific needs is imperative. Timely and effective treatment is crucial in treating MDR TB and XDR TB.

The current gold-standard for drug susceptibility testing (DST) is liquid culture.[4] The most commonly used liquid culture is the mycobacterial growth indicator tube (MGIT) (Becton, Dickinson and Company).[2] The pros of the MGIT are that it produces high specificity and sensitivity.[5] The MGIT also focuses on metabolic indicators of Mtb ($O_2$ consumption) which is helpful to determine viable/nonviable Mtb.[5] Specific design elements of the MGIT are helpful considerations for future TB diagnostics such as culturing with antibiotics to promote specificity and using a metabolic indicator to assess viability.[5] The issues with the MGIT are that the assay is time consuming, labor intensive and requires laboratories with trained individuals and high containment.[5]

The other commonly used TB diagnostic tools have limitations for DST implementation. One of the impediments to using ZN smear microscopy for DST is the fact that the ZN stain can stain dead mycobacteria.[6] Distinguishing between live and dead Mtb is the crux of DSTs and cellular viability. The Gene Xpert MTB/RIF is a useful diagnostic tool for determining RIF resistance in Mtb. This diagnostic tool focuses on known mutations that cause RIF resistance rather than phenotypic signs of drug resistance. The fallback of this design is that it is only able to report on mutations that have clearly been defined as promoting RIF resistance and may miss other signs of RIF resistance. This test only focuses on RIF resistance and does not report on other antibiotic resistance such as isoniazid, ethambutol and pyrazinamide. Neither the ZN stain nor GeneXpert MTB/RIF can distinguish between viable and nonviable Mtb.[6] **There is an urgent need for TB**

**diagnostics that are fast, affordable, sensitive, specific and capable of distinguishing live mycobacteria.**

**Trehalose Probes**

Trehalose probes (Tre-probes) can mediate this issue of labeling nonviable bacteria and non-mycobacteria by focusing on metabolic incorporation into the mycomembrane. Mycobacteria have a unique cell wall structure called the mycomembrane. The mycomembrane is made up of trehalose monomycolates (TMM) that are converted into trehalose dimycolates (TDM) through the Antigen 85 (Ag85) complex.[7] TMM and TDM are thought to be unique to the *Actinomycetales* order, thus excluding other bacteria commonly found in sputum samples.[7] Tre-probes, which leverage the unique properties of the mycomembrane and Ag85 pathway, have shown to be positive tools for Mtb detection.[8]

In 2011, Backus et al. designed a Tre-probe that utilizes the unique properties of the mycomembrane and Ag85 pathway to create a fluorescein-containing trehalose (FITC-trehalose) probe that is incorporated into the mycomembrane.[9] For Mtb *in vitro*, the Ag85 pathway proteins: Ag85A, Ag85B and Ag85C have been reported to produce 41% of the total secreted proteins in culture supernatant, proving the Ag85 pathway a prominent component of mycobacterial cellular metabolism.[9] Interestingly, FITC-glucose demonstrated much lower incorporation potential into Mtb due to the unlikely uptake of the glucose-conjugated probe into the cell through glucose-specific transporters.[9] The superior labeling potential of trehalose-conjugated probes compared to glucose-conjugated probes further demonstrates that the Ag85 pathway plays a crucial role in the labeling of Mtb.

FITC-trehalose is not environment dependent, meaning it is consistently fluorescent.[9] This can cause issues if the trehalose is incorporated endogenously into non-mycobacterial cells and cannot be washed out due to this incorporation. For example in *Eschericia coli* trehalose can be used as a carbon source.[10] To ensure specific FITC-trehalose labeling of mycobacteria, it may be necessary to preprocess the samples to eliminate non-mycobacteria before introducing FITC-trehalose.

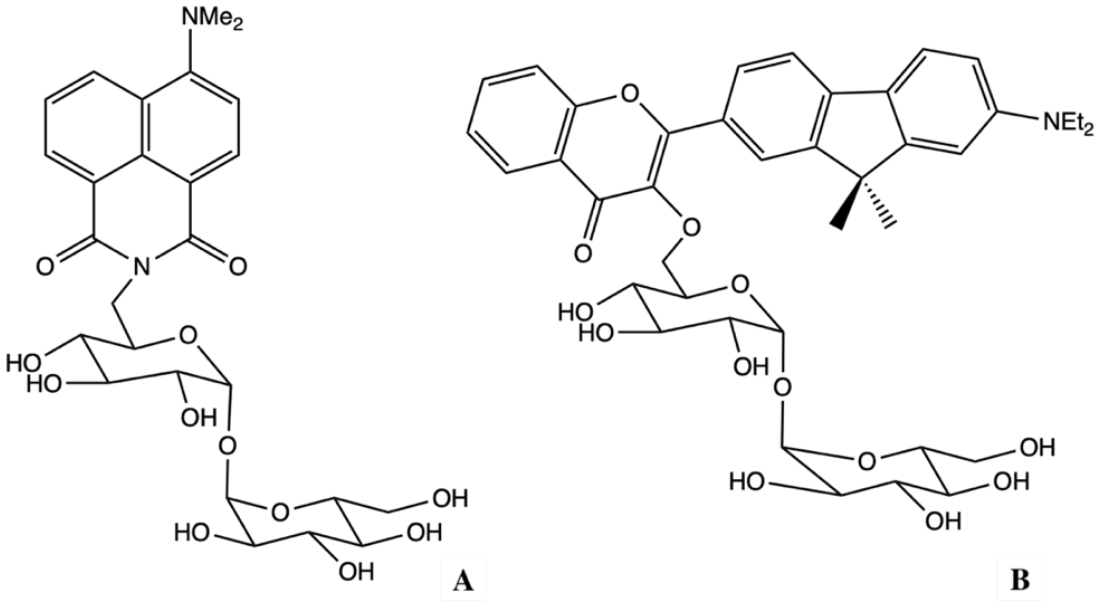


**Figure 1. Schematic of Trehalose probes.**[7,11] **(A)** 4-*N,N*-dimethylamino-1,8-naphthalimide–conjugated trehalose (DMN-Tre) probe. **(B)** 3-Hydroxychromone-conjugated trehalose (3HC-Tre) probe. Figure credit to Lilith Schwartz.

4-*N,N*-dimethylamino-1,8-naphthalimide–conjugated trehalose (DMN-Tre) and 3-Hydroxychromone-conjugated trehalose (3HC-Tre) are solvatochromic probes developed by Kamariza, et al.[7,11] The mechanism of action for the Tre-probes is to be synthesized into TMM, converted into TDM through the Ag85 pathway and thus incorporated into the mycomembrane.[7,11] DMN and 3HC are solvatochromic fluorophores that shows a significant enhancement of

fluorescence when introduced to a hydrophobic environment.[7,11] **These Tre-probes are unique because they are solvatochromic, fluorescing upon incorporation into a hydrophobic environment such as the mycomembrane. This property allows for specific labeling of live, metabolically active mycobacteria.**

The Tre-probes ability to label live, viable mycobacteria can make them a useful tool for DST. A Tre-probe DST would focus on phenotypic indicators, meaning that known mutations would not be required to identify drug resistance. The Tre-probes could be utilized to provide time-sensitive, specific and sensitive drug susceptibility information, to aid in the growing crisis of drug resistance TB. **DMN-Tre and 3HC-Tre, coupled with a 96 well-plate, may produce fast, high-throughput results, testing many different TB drugs at once**.

**Specificity Study**

For this Tre-probe specificity study, we will focus on relevant bacteria found in sputum samples as these samples are commonly used for TB diagnostics and other respiratory tract infections. More than 70% of TB cases are pulmonary TB cases, making sputum a critical clinical specimen for detecting microorganisms in the lungs and respiratory tract.[12,13] Assessing relevant microorganisms in sputum samples is thus essential for robust specificity testing of the Tre-probes.

In a study done by Raghubanshi and Karki, the most common organisms isolated from sputum samples were *Klebsiella pneumoniae* found in 39.5% of sputum samples, *Escherichia coli* in 11.5% and Staphylococci in 11.5%.[14] In a study done by Mansoor et al. the most commonly found microorganisms in a sputum sample were *Klebsiella pneumoniae*, *Streptococcus pneumoniae*, *Pseudomonas aeruginosa*, *Staphylococcus aureus*, *Moraxella catarrhalis* and *Escherichia coli*.[15]

A study focusing on the bacteriology of sputum samples of patients suspected to have TB, reported that the most prominent bacterial isolates from the tested sputum samples were *Pseudomonas species, Klebsiella pneumoniae, Eschericia coli, Streptococcus species, Streptococcus pneumoniae, Staphylococcus aureus* and *Bacillus species*.[16] Additionally, there are several studies world-wide reporting that respiratory tract infections are mainly caused by 11 potent pathogens including *Streptococcus pneumoniae, Klebsiella pneumoniae, Eschericia coli, Staphylococcus aureus and Bacillus species*.[16,17] Based on these findings regarding the composition of human sputum samples, five non-mycobacterial organisms were chosen for this specificity study. **These organisms are *Escherichia coli* (Ec), *Bacillus subtilis* (Bs), *Streptococcus mutans* (Sm), *Staphylococcus aureus* (Staph) and *Klebsiella pneumoniae* (Kp).** In this thesis, Sm was chosen as a BSL1 model organism for *Streptococcus pneumoniae* and *Mycobacterium smegmatis* (Msmeg) was chosen to act as a BSL1 fast-growing model organism for Mtb.

**This thesis will also report on the ability of a plate reader to replace a flow cytometer for fluorescence TB diagnostics.** To achieve the goal of using Tre-probes as diagnostic tools in low-resource settings, it is essential to evaluate cost-effective alternatives to high-end equipment. While a low-cost to mid-range plate reader typically costs between $2,000 and $30,000, a mid-range flow cytometer is significantly more expensive, ranging from $100,000 to $300,000.[18,19] Therefore, it is important to determine whether a plate reader can serve as a sufficient fluorescent reader compared to the more sensitive and costly flow cytometer technology.

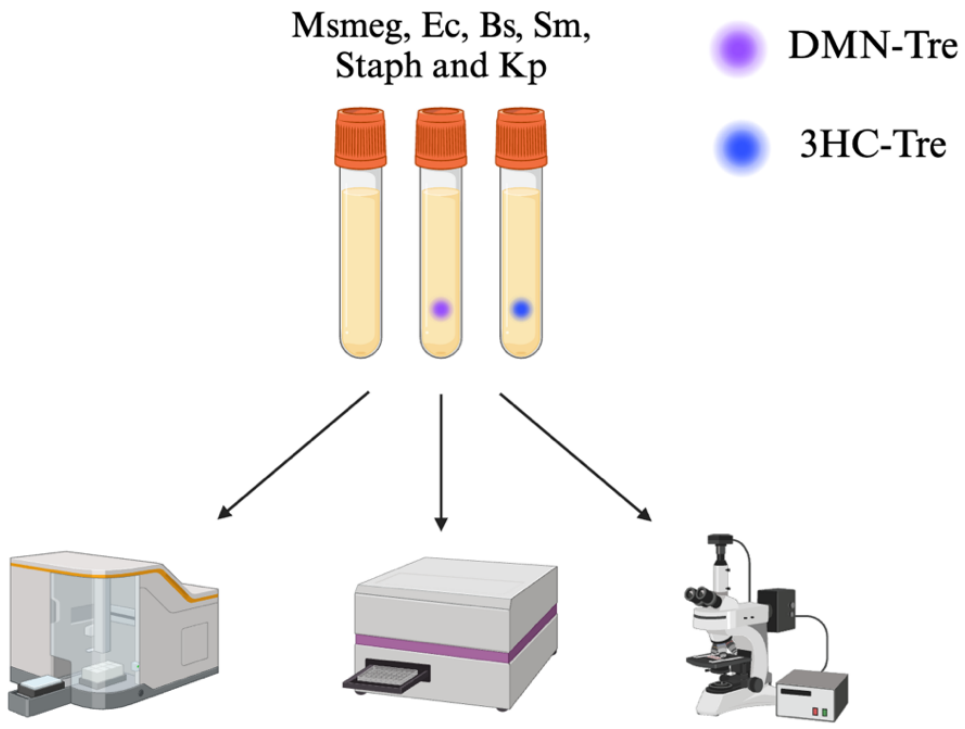


**Figure 2. Schematic representation of specificity workflow**[20]. DMN-Tre and 3HC-Tre labeling of all 6 organisms (Msmeg, Ec, Bs, Sm, Staph and Kp) are tested using three fluorescent detection instruments: flow cytometer, plate reader and microscope.

Specificity will be determined by testing two specific aims. **Aim one focuses on determining specificity of DMN-Tre via flow cytometry, plate reader, and microscopy. Aim two focuses on determining specificity of 3HC-Tre via flow cytometry, plate reader, and microscopy.**

## Chapter 2: Methods

### 7H9 Media Protocol

4.7g of Middlebrook 7H9 broth base (Sigma Aldrich, catalog no. M0178-500G) dissolved in 900mL of DI $H_2O$. 100mL of Oleic Albumin Dextrose Catalase (OADC) (BD BBL™ Middlebrook OADC Enrichment, Fisher Scientific, catalog no. BD212351) added. 10mL of 50% (v/v) glycerol (Sigma Aldrich, catalog no. G2025-500ML) added. 2.5 mL of 20% (v/v) Tween80 (Fisher Scientific, catalog no. BP338-500) added. 50% (v/v) glycerol stocks prepared using equal parts DI $H_2O$ and equal parts glycerol. 20% (v/v) Tween80 stocks prepared using 1:5 ratio of Tween80:DI $H_2O$. Sterilized 7H9 media mixture through a 0.22-µm membrane filter (Corning™ Disposable Sterile Bottle-Top Filters with 0.22µm Membrane, Fisher Scientific, 09-761-112) into an autoclaved bottle. Stored for no more than 3 months at 4℃.

### 7H10 plates for Msmeg

19g of Middlebrook 7H10 agar base (Sigma Aldrich, catalog no. M0303-500G) dissolved in 900 mL of DI $H_2O$. Autoclaved at 121°C for 20 minutes. Agar mixture cooled on bench for 30 minutes with stirring. 100 mL of OADC and 10 mL of 50% (w/v) glycerol added. 7H10 agar mixture poured slowly onto plates. After plates were cooled, they were stored upside down at 4℃ for no more than three months.

### Luria broth plates for Ec and Bs

Dissolve 12.5 g of LB broth base in 500 mL of DI $H_2O$. Mix in 7.5g of agar (Sigma Aldrich, catalog no. 05038-500G). Autoclave at 121℃ for 15 minutes. Stir mixture while cooling. Transfer the mixture to sterile plates. After plates have cooled, store upside down at 4℃.

**Brain heart infusion plates for Sm**

Dissolve 26 g of brain heart infusion agar (Fisher Scientific, catalog no. DF0418-17-7) in 500 mL of DI $H_2O$ and autoclave at 121℃ for 15 minutes. Refer to the Luria broth plate instructions and follow the following steps to determine how to stir, transfer and store.

**Tryptic soy plates for Staph**

Dissolve 20 g of tryptic soy agar (Fisher Scientific, catalog no. DF0369-17-6) in 500mL of DI $H_2O$ and autoclave at 121℃ for 15 minutes. Refer to the Luria broth plate instructions and follow the following steps to determine how to stir, transfer and store.

**Difco nutrient plates for Kp**

Dissolve 4 g of Difco nutrient broth (Fisher Scientific, catalog no. DF0003-17-8) in 500 mL of DI $H_2O$. Mix in 7.5g of agar (Sigma Aldrich, catalog no. 05038-500G). Autoclave at 121℃ for 15 minutes. Refer to the Luria broth plate instructions and follow the following steps to determine how to stir, transfer and store.

**Streaking plates**

Plates brought to room temperature for 10 minutes and marked in 4 quadrants. 5 µL of culture (diluted to less than OD: 0.05) streaked onto each quadrant using sterile inoculation loop. Cultures on plates are grown at 37℃ for 24-48 hours and then parafilmed and stored at 4℃ for no more than 4 weeks.

**Making frozen stocks**

Cultures grown to an OD: 0.8-1 or diluted to this range. 500 µL of culture and 500 µL of 50% (v/v) glycerol aliquoted to 2.0 mL cryogenic vials (Corning, catalog no. 430659) and stored at -80℃.

**Culturing of *M. smegmatis* (Msmeg)**

Colony of Msmeg inoculated in 10mL of 7H9 media (OADC, 50% glycerol, 20% tween80). Msmeg cultures grown for 48 hours in 14 mL culture tubes and then used for designated experiments. If cultures were used after the 48-hour period, 100 µL of Msmeg culture was added to 10 mL of fresh 7H9 media and used within the 24-hour period. Daily care of the cultures entailed spiking 100 µL of previous culture into 10 mL of warmed 7H9 media. Cultures were used for at most five days before bleaching and inoculating a new colony.

**Culturing of *E. coli* (Ec)**

25 g of Luria broth base (Thermo Fisher Scientific, catalog no. 12795027) dissolved in 1000 mL of DI $H_2O$ and autoclaved at 121℃ for 15 minutes. Luria broth stored at 4℃ for no more than 6 months. Luria broth (LB) warmed at 37℃ for 5 minutes before use. Colony of Ec (W1485 strain is a lambda-derivative of *E. coli* strain K-12, ATCC, catalog no. 12435) inoculated in 10mL of LB in 14 mL culture tubes. Ec cultures grown for 24 hours and then used for designated experiments. If cultures were used after the 24-hour period, 100 µL of Ec culture was added to 10 mL of fresh (warmed) LB media and used within the 24-hour period. Daily care of the cultures entailed spiking 100 µL of previous culture into 10 mL of warmed LB broth. Cultures were used for at most five days before bleaching and inoculating a new colony.

**Culturing of *B. subtilis* (Bs)**

Luria broth (LB) warmed at 37℃ for 5 minutes before use. Colony of Bs inoculated in 10mL of LB in 14 mL culture tubes (Thermo Fisher Scientific, catalog no. 1495911B). Bs cultures grown for 24 hours and then used for designated experiments. If cultures were used after the 24 hour period, 100 µL of Bs culture was added to 10 mL of fresh (warmed) LB media and used within the 24 hour period. Daily care of the cultures entailed spiking 100 µL of previous culture into 10 mL of warmed LB broth. Cultures were used for at most five days before bleaching and inoculating a new colony.

**Culturing of *S. mutans (Sm)***

37 g of brain heart infusion broth (Fisher Scientific, catalog no. DF0037178) dissolved in 1000 mL of DI $H_2O$ and autoclaved at 121℃ for 20 minutes. Brain heart infusion broth stored at 4℃ for no more than 6 months. Colony of Sm (strain NCTC 10449, ATCC, catalog no. 25175) inoculated in 10mL of brain heart infusion broth in 14 mL culture tubes. Sm cultures grown for 24 hours and then used for designated experiments. If cultures were used after the 24-hour period, 100 µL of Sm culture was added to 10 mL of fresh brain heart infusion media and used within the 24-hour period. Daily care of the cultures entailed spiking 100 µL of previous culture into 10 mL of brain heart infusion broth. Cultures were used for at most five days before bleaching and inoculating a new colony.

**Culturing of *S. aureus* (Staph)**

30 g of tryptic soy broth (Fisher Scientific, catalog no. DF0369176) dissolved in 1000 mL of DI $H_2O$ and autoclaved at 121℃ for 20 minutes. Tryptic soy broth stored at 4℃ for no more than 6 months. All culturing of BSL2 organism, staph, was done in a biosafety cabinet. Colony of staph

(strain NCTC 8532, ATCC, catalog no. 12600) inoculated in 10mL of tryptic soy broth in T25 non-treated tissue culture flasks (Fisher Scientific, catalog no. FB012933). Staph cultures grown for 24 hours and then used for designated experiments. If cultures were used after the 24-hour period, 100 µL of staph culture was added to 10 mL of fresh tryptic soy broth and used within the 24-hour period.

**Culturing of *K. pneumoniae* (Kp)**

8 g of Difco nutrient broth (Fisher Scientific, catalog no. DF0003-17-8) dissolved in 1000 mL of DI $H_2O$ and autoclaved at 121°C for 20 minutes. Difco nutrient broth stored at 4°C for no more than 6 months. All culturing of BSL2 organism, Kp, was done in a biosafety cabinet. Colony of Kp (strain NCTC 9633, ATCC, catalog no. 13883) inoculated in 10mL of Difco nutrient broth in T25 flasks. Kp cultures grown for 48-72 hours and then used for designated experiments.

**Growth Curves for BSL1**

10 mL cultures diluted to $OD_{600}$: 0.1 using designated media (Msmeg grown in 7H9, Ec and Bs grown in LB and Sm grown in brain heart infusion broth) in 14 mL culture tubes. LB broth warmed before the start of growth curves. At designated time points, cultures were removed from the 37°C shaking incubator and $OD_{600}$ was read using absorbance on the plate reader (SpectraMax iD3 microplate reader) on a 96 well clear, clear bottom plate (ThermoFisher Scientific, catalog no. 267578). Took 4 total readings of each culture respectively (150 µL for each reading) for each time point. Samples were read non-diluted until the last time point where they were diluted by 2x in designated media in order to ensure a more accurate reading of dense cultures. Msmeg and Bs time points (t = 0, 2, 4, 8, 24.5 hours). Ec and Sm time points (t = 0, 2, 3.5, 8, 24.5 hours). 3 biological replicates were done for each organism (Msmeg, Bs, Ec and Sm).

**Growth Curves for BSL2**

12 mL cultures diluted to $OD_{600}$: 0.1 using designated media (staph grown in tryptic soy broth and Kp grown in Difco nutrient broth) in T25 flasks. At designated time points, cultures were removed from the 37℃ non-shaking incubator and $OD_{600}$ was read using absorbance on plate reader on a 96 well clear bottom, clear plate with lid. Took 4 total readings of each culture respectively (150 µL for each reading) for each time point. Samples were read non-diluted for Kp and non-diluted for staph until t = 7.5 which was diluted 2x and t = 24.25 which was diluted 3x to ensure a more accurate reading of dense cultures. Time points were 0, 2, 3.5, 7.5 and 24.25 hours. 3 biological replicates were done for both staph and Kp.

**Labeling and washes for BSL1**

DMN-Tre and 3HC-Tre (OliLux BioSciences) were received lyophilized and then stored in -80℃. The probes were dissolved in DI $H_2O$ to create 20mM DMN-Tre stocks and 1mM 3HC-Tre stocks, stored at -20℃. All organisms (Msmeg, Ec, Bs, and Sm) were diluted to $OD_{600}$ of 0.5 in their respective media (LB broth warmed before use). For each organism there were three samples (unlabeled, DMN-Tre labeled, and 3HC-Tre labeled). 1000 µL transferred to one 1.5 mL Eppendorf tube (Fisher Scientific, catalog no. 21-402-903) as the “unlabeled” sample, 995 µL transferred to one micro-centrifuge tube as the “DMN-Tre" sample and 990 µL transferred to one micro-centrifuge tube as the “3HC-Tre" sample. 5 µL of thawed and mixed 20mM DMN-Tre was added to the DMN-Tre sample (100uM of DMN-Tre in sample) and 10 µL of thawed and mixed 1mM 3HC-Tre was added to the 3HC-Tre sample (10 uM 3HC-Tre in sample). Eppendorf tubes were transferred to 37℃ shaking incubator for 30 minutes. After the 30-minute labeling period, tubes were removed and spun down at 21300 x g for 1 minute (Eppendorf, centrifuge 5420). 950

μL of supernatant was removed (not the full 1000 μL so as not to disrupt the pellet) and the pellet was resuspended in 1000 μL of DPBS (Sigma Aldrich, catalog no. D8662-1L). Tubes were spun down again at 21300 x g for 1 minute. 1000 μL of supernatant was removed and the pellet was resuspended again in 1000 μL in DPBS. Samples were thoroughly pipette mixed and vortexed. 150 μL of sample was transferred to black, black bottom plate (ThermoFisher Scientific, catalog no. 237108) (4 technical replicates) and 75 μL of sample and 75 μL of DPBS was transferred to a clear plate (2x dilution, 4 technical replicates). Fluorescence on the plate reader (SpectraMax iD3 microplate reader) was read at an excitation wavelength of 405 nm and an emission wavelength of 525 nm. Fluorescence on the flow cytometer (BD biosciences flow Accuri cytometer) was read using a 488 nm laser and the FL-1 filter setting indicating FITC emission. All flow data was collected using 100,000 events per sample.

**Labeling and washes for BSL2**

All work with BSL 2 organisms (staph and Kp) were done in a biosafety cabinet. All organisms were diluted to $OD_{600}$ of 0.3 in their respective media. For each organism there were three samples (unlabeled, DMN-Tre labeled, and 3HC-Tre labeled). 3000 μL transferred to one T12.5 flask as the “unlabeled” sample, 2985 μL transferred to one T12.5 flask as the “DMN-Tre" sample and 2970 μL transferred to one T12.5 flask as the “3HC-Tre" sample. 15 μL of thawed and mixed 20mM DMN-Tre was added to the DMN-Tre sample (100uM of DMN-Tre in sample) and 30 μL of thawed and mixed 1mM 3HC-Tre was added to the 3HC-Tre sample (10 uM 3HC-Tre in sample). T12.5 flasks (Fisherbrand™ Surface Treated Sterile Tissue Culture Flasks, Vented Cap, Fisher Scientific, catalog no. FB012933) were transferred to 37°C non-shaking incubator for 30 minutes. After the 30-minute labeling period, flasks were removed and 1000 μL from each flask was transferred to a respective 1.5 mL Eppendorf tube. Eppendorf tubes were spun down at 21300

x g for 1 minute (ThermoScientific ST 8R). 950 µL of supernatant was removed (not the full 1000 µL so as not to disrupt the pellet) and the pellet was resuspended in 1000 µL of 4% formaldehyde (4.5 mL of (stock) into 35.5 mL DPBS). Samples were incubated with formaldehyde for 10 minutes. Tubes were then spun down at 5000 x g for 10 minutes. 1000 µL of supernatant was removed and the pellet was resuspended in 1000 µL in DPBS. Samples were thoroughly pipette mixed and vortexed. Samples were transferred to 96 well plates in the same protocol that was used for labeling and washes for BSL1. Plate reader and flow cytometry fluorescence values were collected in the same way as they were for the labeling and washes for BSL1.

**Labeling and washes with BSL2 controls for Msmeg**

Msmeg was diluted to $OD_{600}$ of 0.3 in 7H9 media. There were three samples (unlabeled, DMN-Tre labeled, and 3HC-Tre labeled). 3000 µL transferred to one T12.5 flask as the “unlabeled” sample, 2985 µL transferred to one T12.5 flask as the “DMN-Tre" sample and 2970 µL transferred to one T12.5 flask as the “3HC-Tre" sample. 15 µL of thawed and mixed 20mM DMN-Tre was added to the DMN-Tre sample (100uM of DMN-Tre in sample) and 30 µL of thawed and mixed 1mM 3HC-Tre was added to the 3HC-Tre sample (10 uM 3HC-Tre in sample). T12.5 flasks were transferred to 37°C non-shaking incubator for 30 minutes. After the 30-minute labeling period, flasks were removed and 1000 µL from each flask was transferred to a respective 1.5 mL Eppendorf tube. Eppendorf tubes were spun down at 21300 x g for 1 minute (Eppendorf, centrifuge 5420). 950 µL of supernatant was removed (not the full 1000 µL so as not to disrupt the pellet) and the pellet was resuspended in 1000 µL of DPBS. Tubes were then spun down again at 21300 x g for 1 minute. 1000 µL of supernatant was removed and the pellet was resuspended in 1000 µL in DPBS. Samples were thoroughly pipette mixed and vortexed. Samples were transferred to 96 well plates in the same protocol that was used for labeling and washes for BSL1. Plate reader and flow cytometry

fluorescence values were collected in the same way as they were for the labeling and washes for BSL1.

**Statistical analysis**

All statistical analysis was performed on GraphPad Prism. T tests were performed using the following parameters: unpaired, parametric and assuming both populations have the same standard deviation (SD). For grouped data it was assumed that samples from each row are from populations with the same SD.

**Microscopy Workflow**

10μL of sample was transferred onto a microscope slide (Fisher Scientific, catalog no. 12-550-133) with an agar pad and clear nail polish was used to stick on the slide cover. Wide-field microscopy (Leica DMIRB/E Inverted Microscope) was performed for all the samples. Image brightness and contrast were edited on FIJI to isolate fluorescence of DMN-Tre and 3HC-Tre labeled Msmeg fluorescence readings and cut out background auto-fluorescence of the Msmeg cells. All CFP channel TIF microscopy images except for Bs images were edited on Fiji is just ImageJ (FIJI) to display brightness/contrast minimum displayed value of 600 and maximum displayed value of 5000. All GFP channel images except for Bs images have a minimum displayed value of 600 and maximum displayed value of 8000. Bs DMN-Tre images edited to 10,000-13,000 (CFP) and 10,000-17,000 (GFP). Corresponding Msmeg microscopy images for Bs images found in SI (Figure S5). Bs 3HC-Tre images edited to 6,200-38,000 (CFP) and 5,700-34,000 (GFP). Corresponding Msmeg microscopy images for Bs images found in SI (Figure S6).

**BLASTP Search**

Msmeg FbpA, FbpB and FbpC proteins corresponding to the Ag85 pathway were sourced from National Center for Biotechnology Information (NCBI). A BLAST-P search was performed on NCBI to determine sequences from Mtb, Ec, Bs, Sm, Staph and Kp that most closely aligned with the respective proteins. These sequences were downloaded and aligned to the original Msmeg protein sequence using Benchling.

The Msmeg FbpA protein sequence used was secreted antigen 85-A FbpA [*Mycolicibacterium smegmatis* (strain ATCC 700084 / mc(2)155) (*Mycobacterium smegmatis*)]. For FbpA the corresponding sequences were WGV39898.1:20-328 diacylglycerol acyltransferase/mycolyltransferase Ag85C [M*ycobacterium tuberculosis*], WP_315663919.1:2-77 alpha/beta hydrolase-fold protein [*Escherichia coli*], WP_248314099.1:3-127 alpha/beta hydrolase family protein [*Streptococcus respiraculi*], W_248314099.1:3-127 alpha/beta hydrolase-fold protein, partial [*Staphylococcus aureus*] and W_305228774.1:1-92 alpha/beta hydrolase family protein, partial [*Klebsiella pneumoniae*].

The Msmeg FbpB protein sequence used was diacylglycerol acyltransferase/mycolyltransferase Ag85B (same strain as FbpA). For FbpB the corresponding sequences were PLV51891.1:1-323 hypothetical protein X011_10290 [*Mycobacterium tuberculosis* variant microti OV254], MDX7415457.1:3-61 alpha/beta hydrolase-fold protein [*Escherichia coli*], WP_165993354.1:41-248 alpha/beta hydrolase family protein [*Streptococcus catagoni*], the same sequence used for FbpA *Staphylococcus aureus* and *Klebsiella pneumoniae.*

The Msmeg FbpC protein sequence used was secreted antigen 85-C FbpC (same strain as FbpA).

For FbpC the corresponding sequences were WP_220020010.1:1-326 diacylglycerol acyltransferase/mycolyltransferase Ag85C [*Mycobacterium tuberculosis*], the same sequence used for FbpB *Eschericia coli*, BAM50882.1:40-104 esterase [Synechocystis sp. PCC 6803] [*Bacillus subtilis* BEST7613J], WP_ 303943537.1:39-241 alpha/beta hydrolase family protein [*Streptococcus intantis*], the same sequence used for FbpA *Staphylococcus aureus* and W_305228774.1:2-92 alpha/beta hydrolase family protein, partial [*Klebsiella pneumoniae*].

## Chapter 3: Results

To understand the growth characteristics of each organism, growth curves of **Msmeg**, **Ec**, **Bs**, **Sm**, **Staph** and **Kp** cultures were first completed. Subsequently, all six organisms were treated with 100 μM of DMN-Tre or 10 μM of 3HC-Tre and compared to corresponding unlabeled cultures. After Tre-probe treatment, all samples were incubated for 30 minutes and then washed twice with DPBS. Fluorescence intensity outputs were measured via flow cytometry, plate reader and microscopy. This section will cover the results of the growth curves and Tre-probe labeling assays in order to determine Tre-probe specificity for mycobacteria.

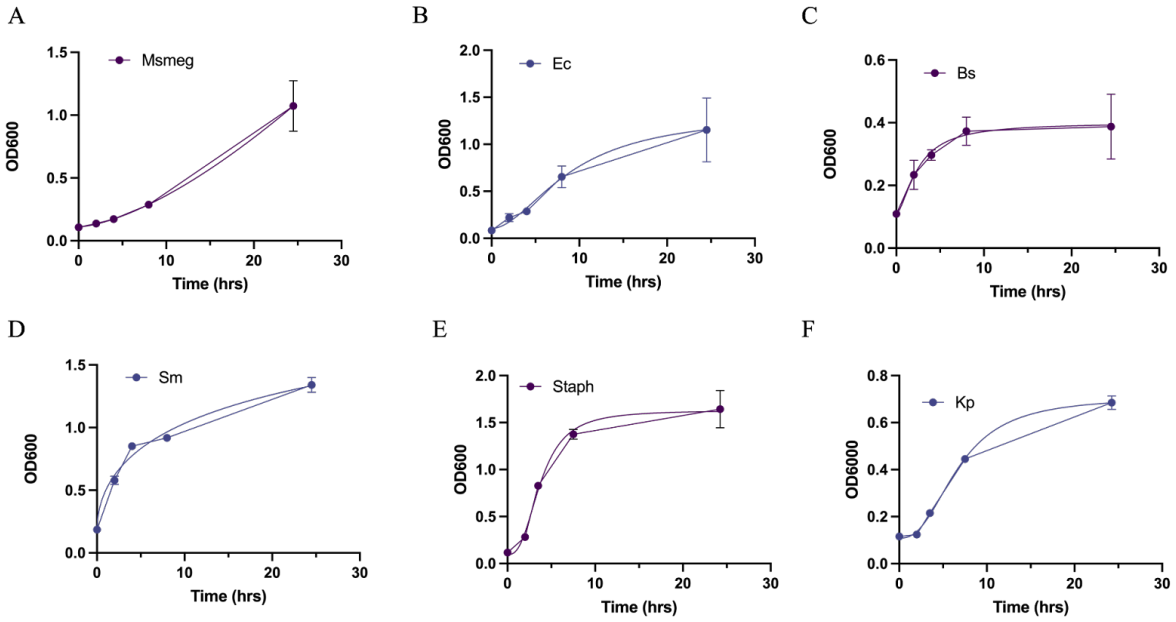


**Figure 3. Growth curves demonstrate exponential growth of all six organisms. (A)** Msmeg, **(B)** Ec, **(C)** Bs, **(D)** Sm, **(E)** Staph and **(F)** Kp cells were grown in 7H9, LB, brain heart infusion broth, tryptic soy broth and Difco nutrient broth respectively. Cultures were diluted to an $OD_{600}$ of 0.1, incubated at 37°C and measurements were taken periodically for about 25 hours. Each graph is representative of three biological replicates. The corresponding lines of best fit were generated through non-linear regression and the equations can be found in Figure S1.

In Figure 3, we successfully demonstrated the exponential phase of growth through growth curves. Growth curve success was attributed to the consistency observed across three biological replicates and the clear demonstration of an exponential phase, as depicted in Figures S2 and S3. The exponential phase was identified by calculating the average $OD_{600}$ readings of the second, third, and fourth time points for each growth curve and fitting an exponential trendline. These time points were selected based on literature precedent, which defines the first phase of growth as the lag phase, the second phase as the exponential phase, the third phase as the stationary phase, and the fourth phase as the death phase.[21] Notably, all R-squared ($R^2$) values for the exponential trendlines exceeded 0.95, except for Sm (0.71) and Staph (0.87), indicating adequate achievement of exponential growth (Figure S3). The Tre-probes serve as metabolic indicators and therefore exhibit higher fluorescence in Msmeg cultures during the exponential phase compared to the stationary phase (Figure S4). With this information, we opted to label cells within the exponential phase at $OD_{600}$ 0.3-0.5 to maximize fluorescence labeling. BSL1 organisms were labeled at $OD_{600}$ 0.5, while BSL2 organisms were labeled at $OD_{600}$ 0.3.

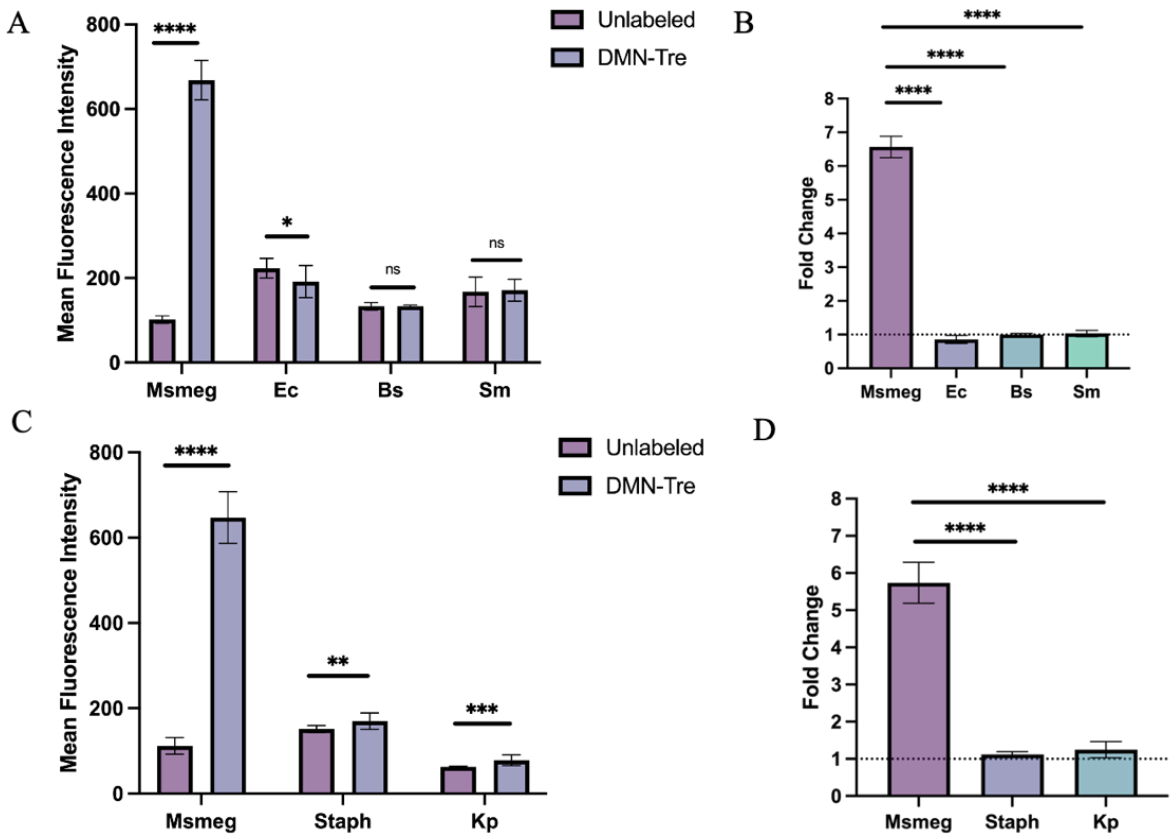


**Figure 4. DMN-Tre labeling is specific to Msmeg by flow cytometry.** (**A)** and (**C)** Flow cytometry mean-FITC taken using a 488 nm laser. All cultures diluted to $OD_{600}$: 0.5, treated with or without 100 μM DMN-Tre depending on the sample and incubated for 30 minutes. (**B)** and **(D)** Fold change was calculated as the mean-FITC measurements of the DMN-Tre labeled samples divided by the average unlabeled mean-FITC measurement for each corresponding organism. All graphs are representative of three biological replicates. All p-values were calculated on GraphPad Prism using an unpaired, parametric test. (****P < 0.0001, ***P < 0.001, **P < 0.01, *P < 0.1, ns > 0.1).

We first designed an experiment to determine whether DMN-Tre can specifically label **Msmeg** cells and distinguish them from cells of other bacterial genera. We performed DMN-Tre labeling of cultures of **Msmeg**, **Ec**, **Bs**, **Sm**, **Staph** and **Kp**. The labeled bacteria were then analyzed using a flow cytometer to measure mean-FITC values, used as a quantitative measure of DMN-Tre incorporation into the cells. The mean-FITC values for **Msmeg**, **Ec**, **Bs** and **Sm** were 6.57, 0.85, 1.00 and 1.03 respectively, showing a significant difference between Msmeg and non-

mycobacteria (Figure 4a). The fold changes (FCs) in mean-FITC values for **Msmeg**, **Staph** and **Kp** were 5.74, 1.12 and 1.25 respectively, again demonstrating a distinct difference between Msmeg and non-mycobacteria (Figure 4d). **Our findings demonstrate that DMN-Tre labeling, as measured by mean-FITC values on the flow cytometer, can be used as a specific marker for identifying Msmeg cells among various bacterial genera.**

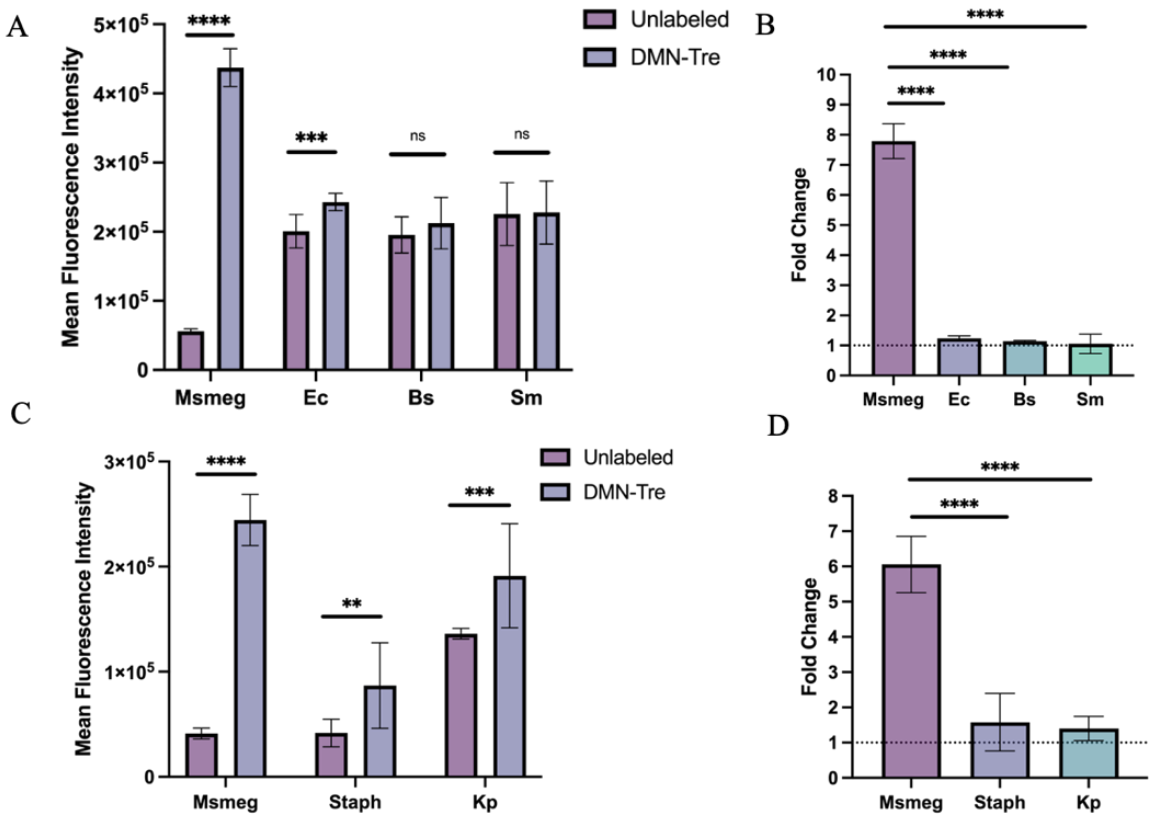


**Figure 5. DMN-Tre labeling is specific to Msmeg by plate reader.** (**A)** and (**C)** Plate reader fluorescence data taken using excitation wavelength of 405 nm and emission wavelength of 525 nm. All cultures diluted to $OD_{600}$: 0.5 (**A**) and 0.3 (**C**) treated with or without 100 µM DMN-Tre depending on the sample and incubated for 30 minutes. (**B)** and (**D)** FC was calculated as the fluorescence measurement of the DMN-Tre labeled samples divided by the average unlabeled fluorescence measurement for each corresponding organism. All graphs are representative of three biological replicates. All p-values calculated on GraphPad Prism using an unpaired, parametric test. (****P < 0.0001, ***P < 0.001, **P < 0.01, *P < 0.1, ns > 0.1).

Next, we assessed DMN-Tre labeling of **Msmeg**, **Ec**, **Bs**, **Sm**, **Staph** and **Kp** by comparing fluorescence readings of unlabeled and DMN-Tre labeled cells. In this assay we aimed to determine whether a plate reader can serve as a cheaper alternative to flow cytometry for diagnostic purposes by comparing fluorescence readings of DMN-Tre labeled bacteria. The same samples analyzed on the flow cytometer in Figure 4 were also evaluated using a plate reader.

The FCs for **Msmeg**, **Ec**, **Bs** and **Sm** were 7.79, 1.24, 1.14 and 1.06 respectively, indicating a significantly higher difference in DMN-Tre labeled Msmeg compared to other organisms (Figure 5B). It is important to point out that the background fluorescence of unlabeled **Ec**, **Bs** and **Sm** cells are more fluorescent than unlabeled Msmeg cells by a factor of 3.5-4.0. The FCs of **Msmeg**, **Staph** and **Kp** are 6.06, 1.58 and 1.40 (Figure 5D). The unlabeled Staph values compared to unlabeled Msmeg are nearly the same (factor of 1.02, SD: 0.25) and the DMN-Tre labeled Staph cells show lower fluorescence values than DMN-Tre labeled Msmeg. However, the unlabeled Kp values compared to Msmeg show a greater difference (factor of 3.33, SD: 0.29) and the DMN-Tre labeled Kp cells do not show distinctly lower fluorescence values than DMN-Tre labeled Msmeg (p-value of 0.0041, **P).

The plate reader indicates that DMN-Tre selectively labels Msmeg, as evidenced by higher FCs in fluorescence compared to other bacteria. However, due to high autofluorescence of some organisms, the plate reader may not be sensitive enough to detect subtle differences in fluorescence values, particularly between DMN-Tre labeled Msmeg and Kp. **Our findings suggest that while DMN-Tre selectively labels Msmeg on the plate reader, the sensitivity of the plate reader may cause diagnostic challenges.**

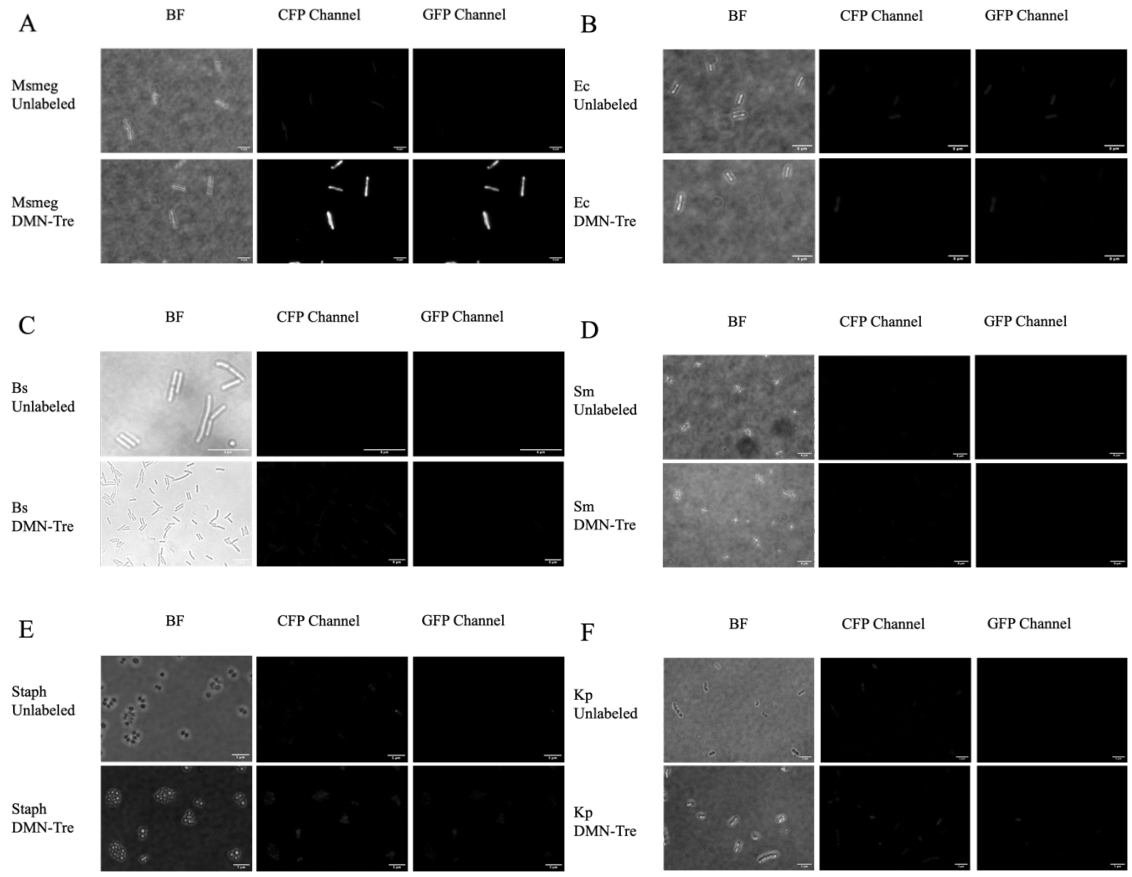


**Figure 6. DMN-Tre labeling is specific to Msmeg by microscopy.** All cultures diluted to $OD_{600}$: 0.5 **(A)**, **(B)**, **(C)** and **(D)**, and 0.3 (**E**) and **(F)** treated with or without 100 µM DMN-Tre depending on the sample and incubated for 30 minutes. Samples were diluted and then streaked onto microscope slides on top of agar pads. **(A)**, **(B)**, **(D)**, **(E)** and **(F)** images taken with 100x objective on Leica wide-field microscope. **(C)** 160x objective used for Bs unlabeled images and 60x objective used for DMN-Tre labeled Bs images. Scale bar: 8 µm (Msmeg, Ec, Bs, Sm images) and 5 µm (Staph and Kp images).

Next, we assessed specificity of DMN-Tre using microscopy. As outlined in the introduction, microscopy is a commonly used TB diagnostic tool. Here, we compare unlabeled and DMN-Tre labeled microscopy images from all six organisms. We used FIJI to uniformly edit out the background autofluorescence of the cells and focus on the fluorescence from DMN-Tre labeling. Images of the non-mycobacteria organisms were edited in the same way as the Msmeg images in

order to standardize the results. DMN-Tre labeled **Msmeg** cells clearly show fluorescence above the autofluorescence values of any of the unlabeled organism images (figure 6a). The non-mycobacteria organisms **Ec**, **Bs**, **Sm**, **Staph** and **Kp** showed no significant fluorescence (figures 6b-6f). The microscopy images confirm that DMN-Tre specifically labels Msmeg cells, as evidenced by the fluorescence observed only in DMN-Tre labeled Msmeg samples and not in the other bacterial samples. **Our microscopy findings support the conclusion that DMN-Tre labeling is specific to Msmeg, providing visual confirmation of the labeling specificity observed on the flow cytometer and plate reader.**

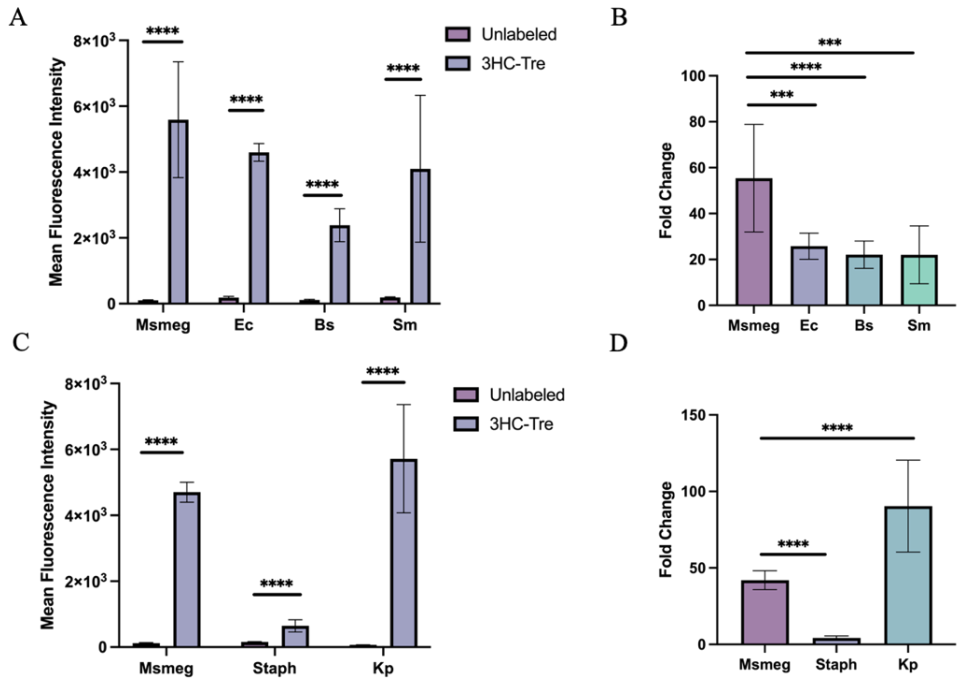


**Figure 7. 3HC-Tre labeling is not specific to Msmeg by flow cytometry.** (**A)** and (**C)** Flow cytometry mean-FITC taken using a 488 nm laser. All cultures diluted to $OD_{600}$: 0.5, treated with or without 10 μM 3HC-Tre depending on the sample and incubated for 30 minutes. (**B)** and **(D)** FC was calculated as the mean-FITC measurements of the 3HC-Tre labeled samples divided by the average unlabeled mean-FITC measurement for each corresponding organism. All graphs are representative of three biological replicates. All p-values were calculated on GraphPad Prism using an unpaired, parametric test. (****P < 0.0001, ***P < 0.001, **P < 0.01, *P < 0.1, ns > 0.1).

We then sought to determine specificity of 3HC-Tre labeling by flow cytometry across different bacterial genera and determine whether it demonstrates specificity towards mycobacteria. We performed 3HC-Tre labeling on cultures of **Msmeg**, **Ec**, **Bs**, **Sm**, **Staph** and **Kp**. We analyzed the flow cytometry mean-FITC measurements to determine specificity. 3HC-Tre labeling of **Msmeg, Ec, Bs and Sm** (figure 7a) shows significant mean-FITC values greater than unlabeled samples (all p-values > 0.0001). The FCs of **Msmeg**, **Ec**, **Bs** and **Sm** are 55.41, 25.80, 22.11 and 22.03 (figure 7b). Staph and Kp also show labeling significantly above the unlabeled control samples (figure 7c) with FCs of 42.00, 4.25 and 90.40 for **Msmeg**, **Staph** and **Kp** respectively (figure 7d). Flow cytometry data indicate that 3HC-Tre labels all six organisms significantly above the unlabeled controls. The FCs demonstrate clear labeling of each organism and does not indicate specificity towards mycobacteria, as non-mycobacterial species also showed significant labeling. **Our findings suggest that while 3HC-Tre effectively labels a variety of bacteria, it lacks specificity towards mycobacteria, as evidenced by significant labeling across different genera.**

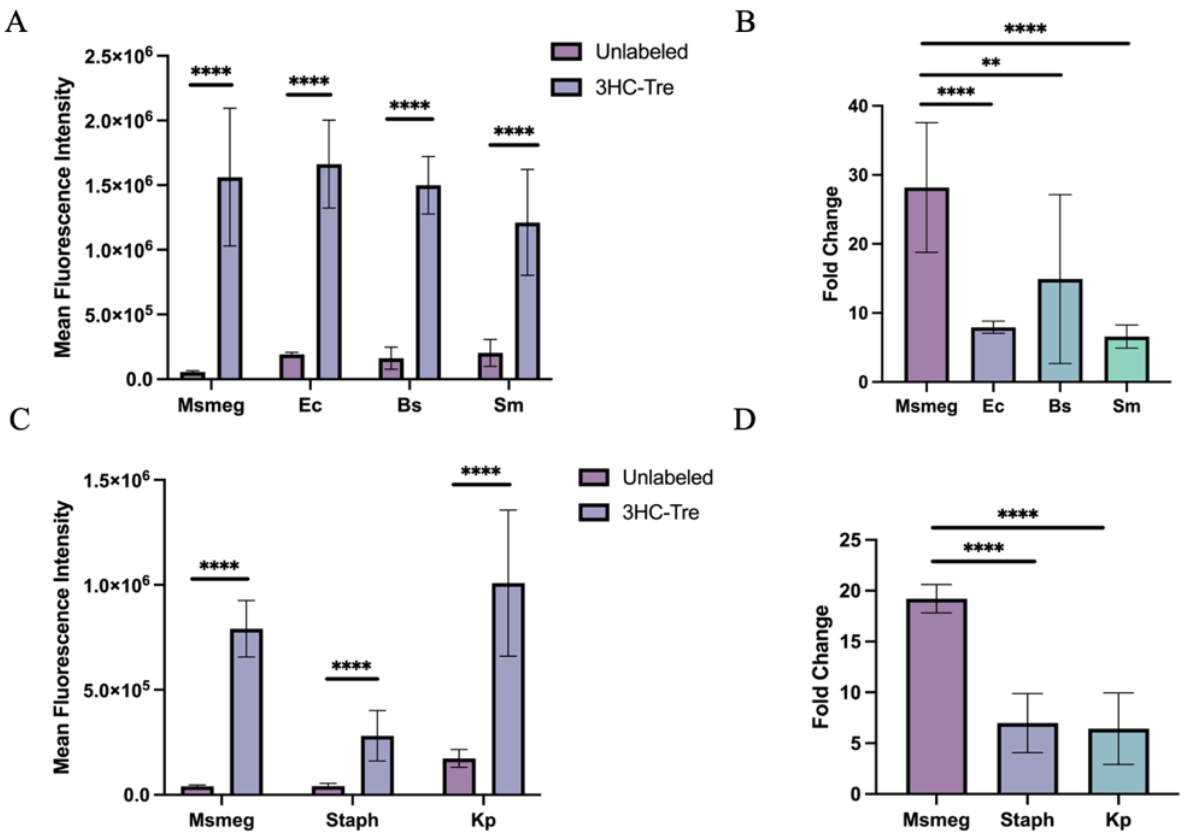


**Figure 8. 3HC-Tre labeling is not specific to Msmeg by plate reader.** (**A)** and (**C)** Plate reader fluorescence data taken using excitation wavelength of 405 nm and emission wavelength of 525 nm. All cultures diluted to $OD_{600}$: 0.5 (**A**) and 0.3 (**C**) treated with or without 10 μM 3HC-Tre depending on the sample and incubated for 30 minutes. (**B)** and (**D)** FC was calculated as the fluorescence measurement of the 3HC-Tre labeled samples divided by the average unlabeled fluorescence measurement for each corresponding organism. All graphs are representative of three biological replicates. All p-values were calculated on GraphPad Prism using an unpaired, parametric test. (****P < 0.0001, ***P < 0.001, **P < 0.01, *P < 0.1, ns > 0.1).

Next, we assessed 3HC-Tre labeling on the plate reader to further assess 3HC-Tre specificity (Figure 8). The same 3HC-Tre labeled samples used for flow cytometry analysis were used to determine plate reader specificity results. Significantly high fluorescence values are observed for all labeled organisms compared to unlabeled controls (Figures 8A and 8C). Staph displays lower fluorescence values compared to the other species but still shows significant labeling (Figures 8C

and 8D). Although the FC for Msmeg appears to be higher than **Ec**, **Bs**, **Sm** and **Kp** this is likely attributed to **Msmeg** cells being lower in fluorescence by factors of 3.0-3.5. Differences in FC may attributed to different levels of 3HC-Tre labeling and variations in autofluorescence of each organism. **These plate reader results reinforce the conclusions made through flow cytometry, 3HC-Tre labels a variety of organisms and does not show specificity towards mycobacteria.**

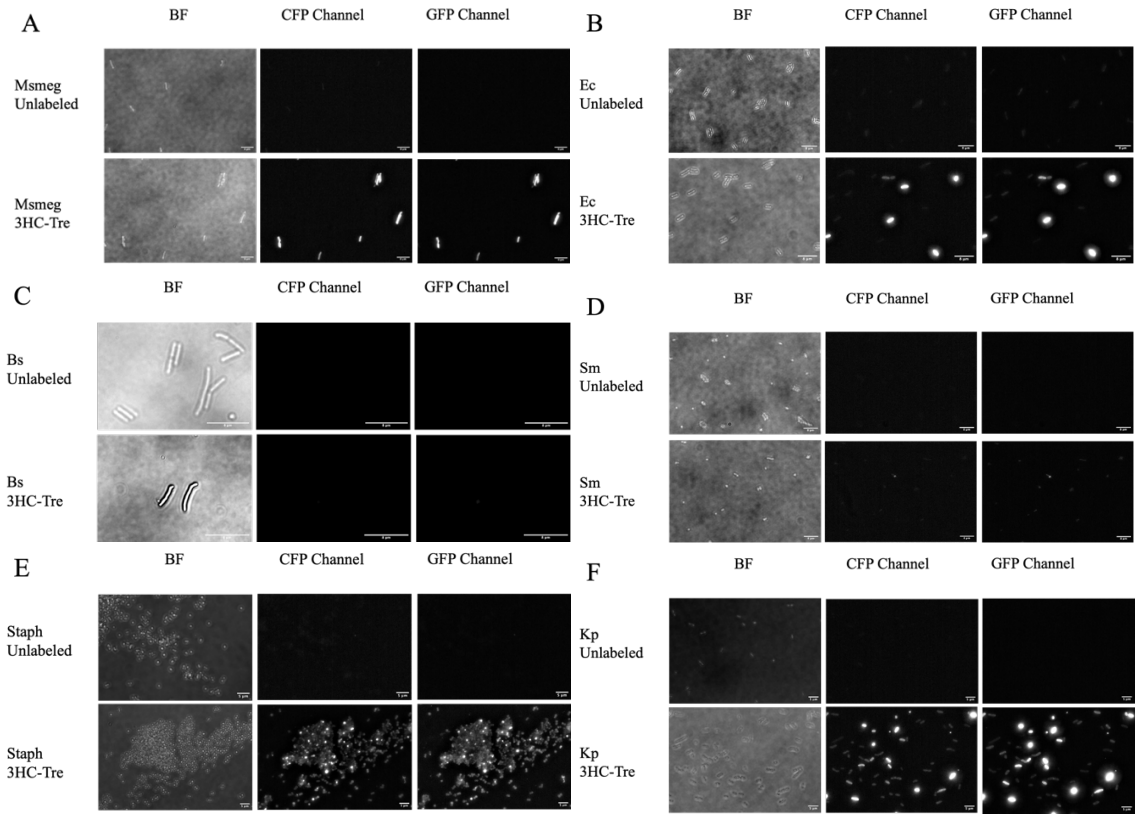


**Figure 9. 3HC-Tre labeling is not specific to Msmeg by microscopy.** All cultures diluted to $OD_{600}$: 0.5 **(A)**, **(B)**, **(C)** and **(D)**, and 0.3 (**E**) and **(F)** treated with or without 10 μM 3HC-Tre depending on the sample and incubated for 30 minutes. Samples were diluted and then streaked onto microscope slides on top of agar pads. **(A)**, **(B)**, **(D)**, **(E)** and **(F)** images taken with 60x objective on Leica wide-field microscope. **(C)** 160x objective used for Bs images. Scale bar: 8 μm (Msmeg, Ec, Bs, Sm images) and 5 μm (Staph and Kp images).

Lastly, we performed microscopy to determine 3HC-Tre probe specificity. Microscopy images were taken on a Leica wide-field microscope and processed uniformly using FIJI. The 3HC-Tre labeled Msmeg, Ec, Staph and Kp show high fluorescence above background fluorescence of unlabeled bacteria (Figures 9A, 9B, 9E and 9F). Microscopy images of 3HC-Tre labeled Bs and Sm do not show fluorescence over unlabeled bacteria autofluorescence (Figures 9C and 9D). In the 3HC-Tre labeled Staph and Kp microscopy images some cells appear to be more labeled than others (Figures 9E and 9F).

Further research is needed to determine the consistency of 3HC-Tre labeling. However, this inconsistency in levels of labeling may be a cause of the noticeably larger error bars in 3HC-Tre labeling compared to DMN-Tre labeling. It is also interesting to note that 3HC-Tre labeled Staph shows more cells with dimmer fluorescent values compared to Msmeg (Figures 9A and 9E). This is congruent with the fluorescence readings on the flow cytometer and plate reader that show lower fluorescence readings compared to the other organisms (Figures 7C and 8C). Microscopy of 3HC-Tre labeled organisms showed labeling of **Msmeg** and **Ec**, as well as differential fluorescence intensity of **Staph** and **Kp**. **Bs** and **Sm** did not demonstrate fluorescent labeling. Further tests are required to determine 3HC-Tre specificity through microscopy.

## Chapter 4: Discussion

One of the over-arching goals of this project is to determine whether a plate reader can serve as a sufficient fluorescent reader compared to the more expensive flow cytometer technology. In this section, we will assess the similarity of fluorescent results obtained using both the plate reader and flow cytometer and discuss whether the plate reader can be considered a low-cost, accessible TB diagnostic alternative.

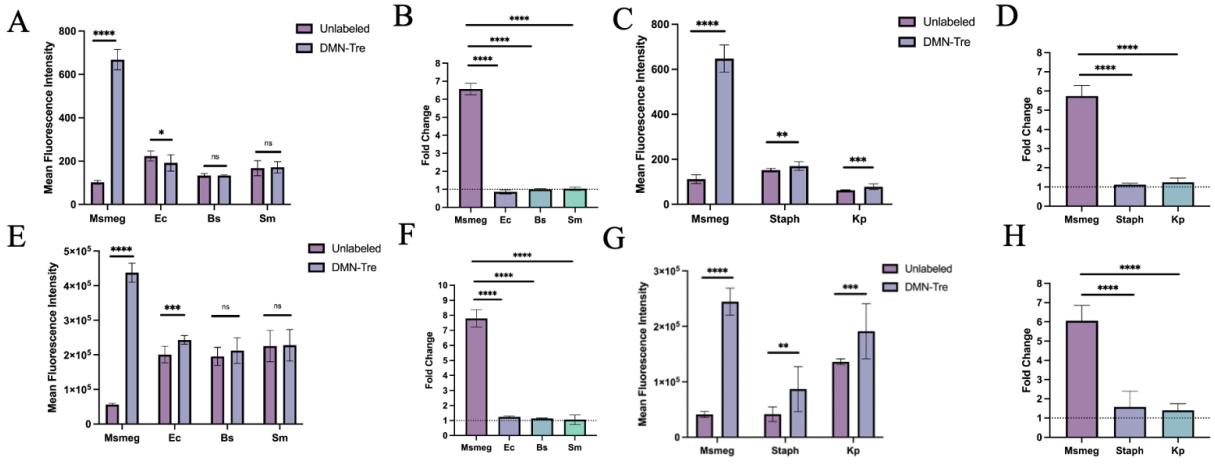


**Figure 10. DMN-Tre labeling is specific by flow cytometry and plate reader**. **(A)** and **(C)** Flow cytometer mean-FITC results for DMN-Tre labeled and unlabeled samples **(B)** and **(D)** FC of flow cytometer mean-FITC DMN-Tre labeled samples/average mean-FITC for unlabeled samples. **(E)** and **(G)** Plate reader fluorescence values for DMN-Tre labeled and unlabeled samples. **(F)** and **(H)** FC of plate reader fluorescence values of DMN-Tre labeled samples/average fluorescence values for unlabeled samples.

The results of DMN-Tre labeling using both the plate reader and flow cytometer are presented in Figure 10. These results show that DMN-Tre labeling of Msmeg is significantly higher than that of any other organisms tested. Background fluorescence of unlabeled Ec, Bs, and Sm is higher on both the flow cytometer and the plate reader. As shown in Figure 10B, the flow cytometry data

confirm that DMN-Tre selectively labels mycobacteria, with only limited fluorescence increases in other organisms.

However, it is important to note the FC of average DMN-Tre labeling of Msmeg compared to Ec, Bs, and Sm. On the flow cytometer, these FCs are 3.56, 5.00, and 4.02 (with SDs of 0.42, 0.30, and 0.94, respectively). On the plate reader, the FCs are 1.80, 2.10, and 2.01 (with SDs of 0.29, 0.52, and 0.24, respectively). These results indicate that although DMN-Tre demonstrates specificity on both devices, the lower sensitivity of the plate reader results in a smaller difference between DMN-Tre labeled Msmeg and other organisms.

Plate readers are substantially cheaper than flow cytometers and enable accessible diagnostic tools. However, our results suggest that plate readers are more significantly affected by varying autofluorescence between different organisms. The issue of high autofluorescence of other bacterial samples in sputum could be solved through a few solutions. (1) One would be that the protocol for diagnostics would involve one sample that is unlabeled with all the bacteria naturally present in the sputum sample and the other sample would be a DMN-Tre labeled sample of the same sputum sample. This way, the change in fluorescence output is known to be a result of the DMN-Tre labeling of mycobacteria. This allows the patient's own sputum sample to be the benchmark fluorescence output. (2) Another solution to this issue of lower plate reader sensitivity would be to process the samples with *N*-acetyl-l-cysteine–sodium hydroxide (NALC-NaOH) to decontaminate the sample of any bacteria that is not mycobacteria. This preprocessing method is commonly used in mycobacteria diagnostics to isolate mycobacteria.[22]

Autofluorescence appears to vary by a factor up to four times among the different organisms tested in this thesis. Various endogenous molecules can influence the autofluorescence properties of different cells, including aromatic amino acids, NAD(P)H, flavins and lipofuscins.[23] Flavins, which often attach to proteins and enzymes and act as cofactors, can be excited at 488 nm.[23,24]

A study by Yang et al. examined the autofluorescence of different bacterial organisms with a 488 nm flow cytometer laser. The study found that Staph had the lowest autofluorescence and Bs had the highest autofluorescence.[23] The organisms tested were Bs, Ec, *M. lysodeikticus*, *Pseudomonas aeruginosa*, *Vibrio alginolyticus*, *Vibrio harveyi* and Staph.[23] The fluorescence results from our 488nm laser flow cytometer and plate reader (Figure 10) align well with the findings of Yang et al., confirming that Staph has low autofluorescence and Bs has comparatively high autofluorescence.

Many internal properties of bacterial species likely contribute to differences in autofluorescence. The Yang et al. study provides one explanation for the variation in autofluorescence among different organisms.

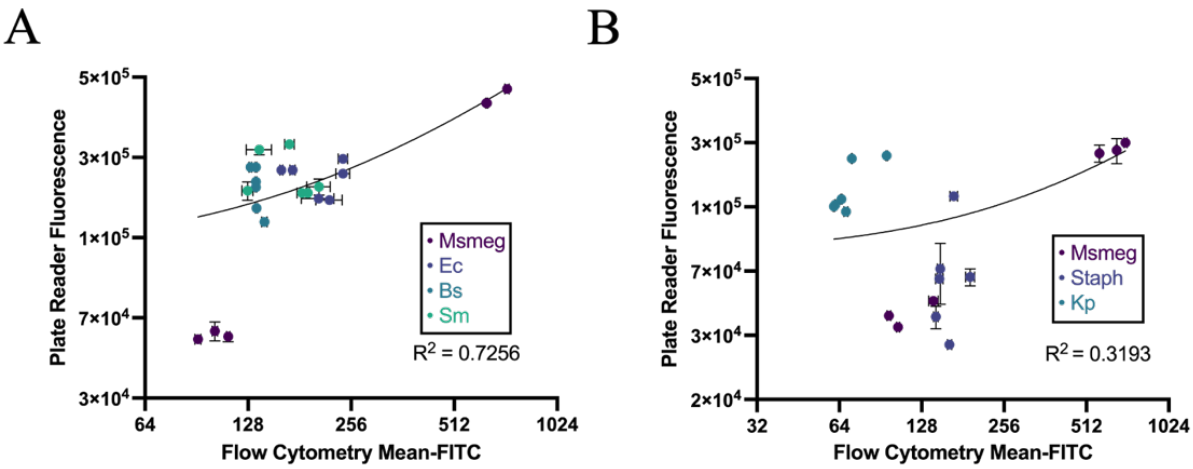


**Figure 11. Low-correlation between DMN-Tre labeled mean-FITC from flow cytometer and fluorescence values from plate reader. (A)** Plate Reader Fluorescence vs. Flow Cytometry Mean-FITC for Msmeg, Ec, Bs and Sm (unlabeled and DMN-Tre labeled samples). **(B)** Plate Reader Fluorescence vs. Flow Cytometry Mean-FITC for Msmeg, Staph and Kp (unlabeled and DMN-Tre labeled samples). Flow cytometry mean-FITC graphed on x-axis with horizontal error bars corresponding to SDs. Plate reader fluorescence graphed on y-axis with vertical error bars referring to corresponding SDs. Simple linear regression and corresponding $R^2$ values calculated using GraphPad Prism.

In order to further test the correlation between the flow cytometer and plate reader, we created a correlation graph comparing the fluorescence readings from both instruments. Simple linear regression and $R^2$ values were calculated to quantify the relationship. Our findings revealed that the BSL1 organism correlation plot exhibited a moderately strong correlation, suggesting a reasonable level of agreement between the two measurement methods (Figure 11a). In contrast, the BSL2 organism correlation plot showed a very poor correlation, indicating a significant discrepancy between the readings from the plate reader and the flow cytometer for these organisms (Figure 11b). With this data, we concluded that there is not sufficient correlation between the plate

reader and flow cytometer, particularly for BSL2 organisms, implying that these two methods may not be directly interchangeable for all bacterial species.

Another important consideration is our demonstration that microscopy is an effective tool for distinguishing between DMN-Tre labeled mycobacteria and non-mycobacteria. Although microscopy does not offer the high throughput capabilities of some other diagnostic methods, it remains a widely used and highly relevant tool for TB diagnosis, especially in low-resource settings.[2] The capacity to distinguish mycobacteria emphasizes the significance of microscopy in diagnostic workflows, especially in environments where resources and access to more advanced technology may be limited.

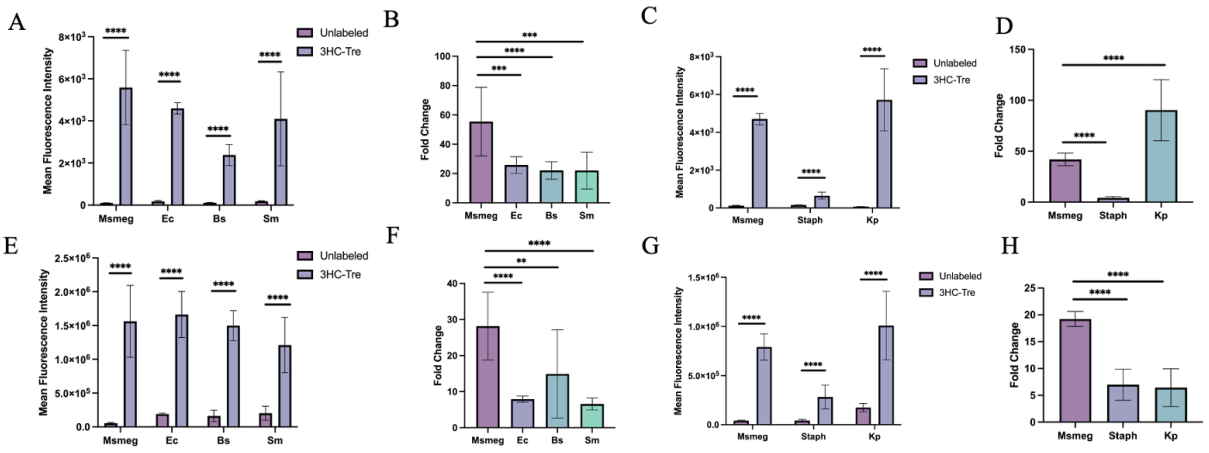


**Figure 12. 3HC-Tre labeling is not specific by flow cytometry or plate reader**. **(A)** and **(C)** Flow cytometer mean-FITC results for 3HC-Tre labeled and unlabeled samples **(B)** and **(D)** FC of flow cytometer mean-FITC 3HC-Tre labeled samples/average mean-FITC for unlabeled samples. **(E)** and **(G)** Plate reader fluorescence values for 3HC-Tre labeled and unlabeled samples. **(F)** and **(H)** FC of plate reader fluorescence values of 3HC-Tre labeled samples/average fluorescence values for unlabeled samples.

On both the plate reader and the flow cytometer 3HC-Tre demonstrates statistically significant labeling of all six organisms (Figure 12). Although Staph shows significantly lower fluorescent

values as compared to Msmeg, these 3HC-Tre labeled fluorescence values still show statistically significant differences compared to unlabeled Staph (Figure 12E and 12G).

The 3HC-Tre microscopy results for Bs and Sm are not consistent with flow cytometry and plate reader fluorescence readings that show significant labeling of 3HC-Tre labeled Bs and Sm (Figures 9C, 9D, 12A and 12E). Clumped 3HC-Tre labeled Bs cells show slight fluorescence over background (Figure S6). This could be due to the 3HC-Tre probe getting stuck between the cells and fluorescing, even though it has not been incorporated into the cell. It could also be a result of the clumped cells having higher background auto-fluorescence compared to individual cells.

The 3HC-Tre microscopy results for Sm and Kp does not demonstrate uniform fluorescence intensity among different cells. It is possible that some of the cells are labeled more than others or that some of the cells fell through the pores of the agar pad and are therefore lower on the plane, leading to less fluorescence. Interestingly, Staph and Kp were the only cells that were fixed with 4% formaldehyde before being imaged.

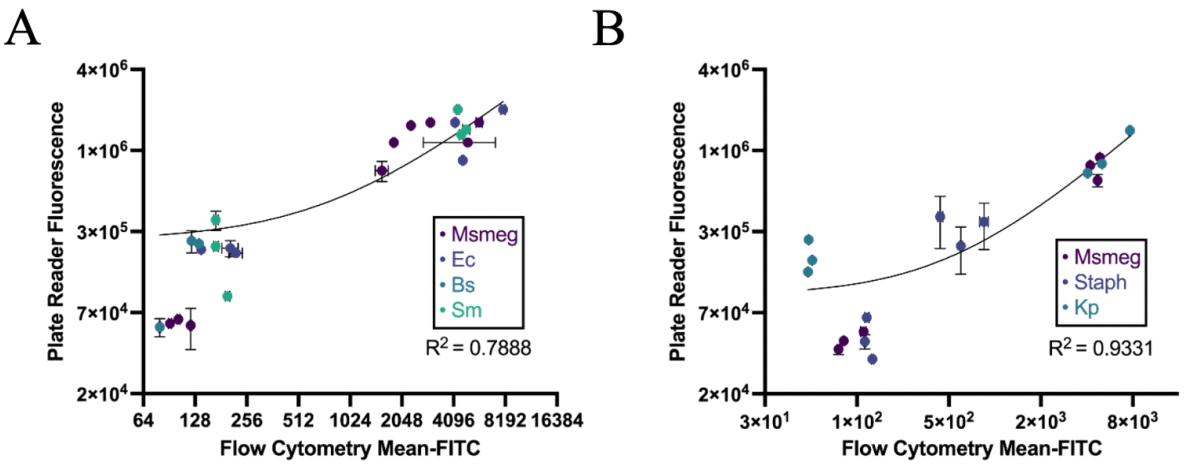


**Figure 13. Moderate-correlation between 3HC-Tre labeled mean-FITC from flow cytometer and fluorescence values from plate reader. (A)** Plate Reader Fluorescence vs. Flow Cytometry Mean-FITC for Msmeg, Ec, Bs and Sm (unlabeled and 3HC-Tre labeled samples). **(B)** Plate Reader Fluorescence vs. Flow Cytometry Mean-FITC for Msmeg, Staph and Kp (unlabeled and 3HC-Tre labeled samples). Flow cytometry mean-FITC graphed on x-axis with horizontal error bars corresponding to SDs. Plate reader fluorescence graphed on y-axis with vertical error bars referring to corresponding SDs. Simple linear regression and corresponding $R^2$ values calculated using GraphPad Prism.

Upon comparing the $R^2$ results of Figure 11 with Figure 13, it becomes evident that a brighter solvatochromic dye, such as 3HC-Tre, may effectively mitigate the issue of lower sensitivity observed on the plate reader. Despite its brighter fluorescence, our findings reveal a critical drawback: the lack of specificity of the 3HC-Tre probe for mycobacteria. If 3HC-Tre proves to offer higher sensitivity than traditional methods like ZN staining, lower cost than Gene Xpert, and faster turnaround time than MGIT, it could still be a valuable diagnostic tool for TB despite its low specificity. Implementing a preprocessing NALC-NaOH decontamination protocol may be worthwhile in order to mitigate the issue of low specificity.[22]

We aimed to find out whether homologous proteins in the other bacterial genera could account for the observed high fluorescence values from 3HC-Tre labeled cells. The development of Tre-probes are rooted in the unique biological mechanism of trehalose incorporation into the mycomembrane.[25] This process of trehalose mycolation and addition into the mycomembrane as trehalose dimycolates (TDM) is carried out by the Antigen 85 (Ag85) pathway. The key proteins associated with this pathway are FbpA, FbpB and FbpC.[9] The mechanism of action for Tre probe labeling via Ag 85 leverages their ability to be mycolated and incorporated into the mycomembrane as trehalose dimycolates (TDM).[7] We conducted a National Center for Biotechnology Information (NCBI) BLASTP searches to determine if there are homologous proteins that may carry out functions similar to this pathway in Mtb, Ec, Bs, Sm, Staph and Kp. **These investigations aimed to determine if there are any homologous proteins that might contribute to the significant fluorescence values across different bacteria genera.**

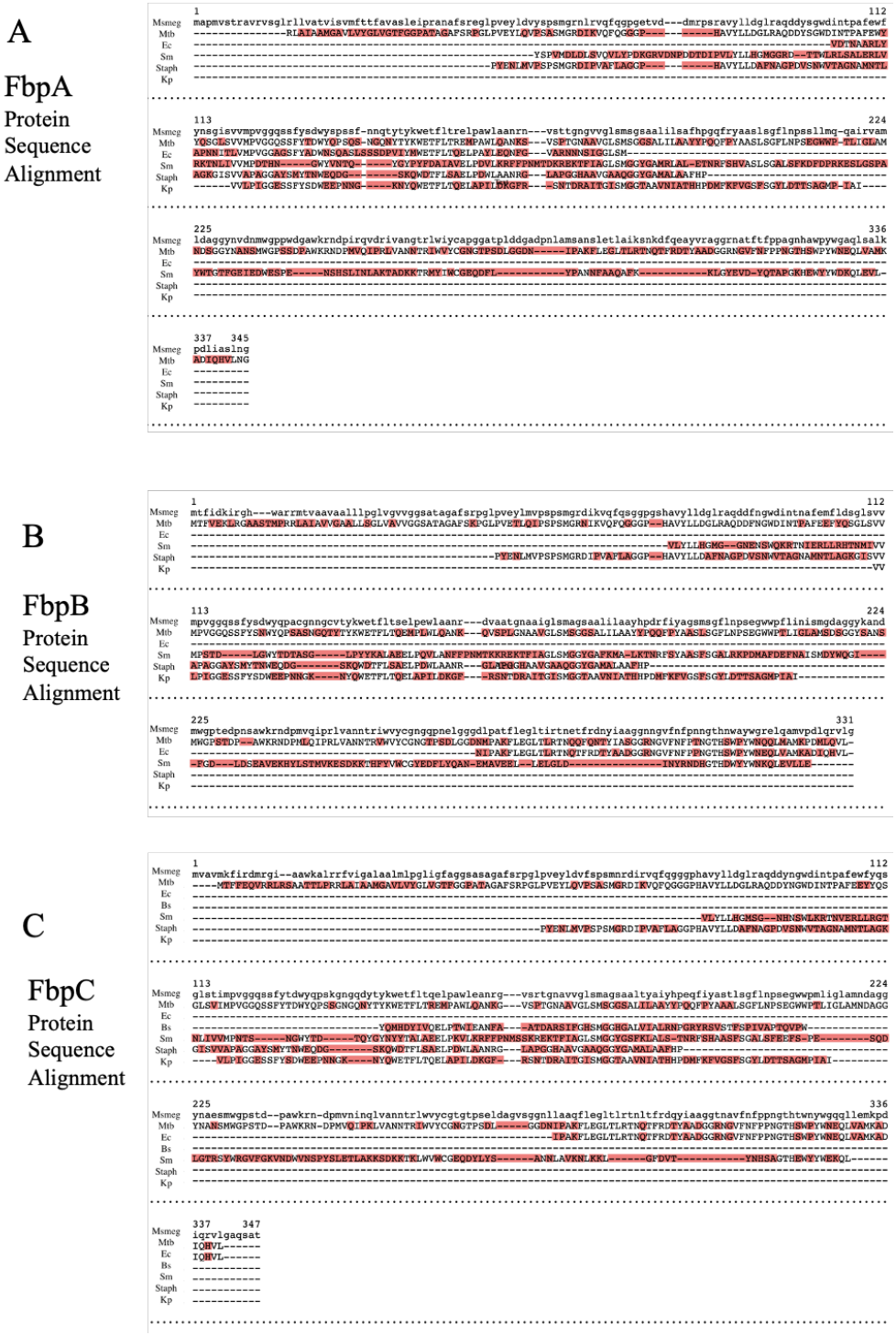


**Figure 14. BLASTP search of Msmeg FbpA, FbpB and FbpC proteins shows limited protein homology for Ec, Bs, Sm, Staph and Kp. (A), (B)** and **(C)** BLASTP Msmeg FbpA, FbpB and FbpC protein sequenced searched for in Mtb, Ec, Bs, Sm, Staph and Kp. Sequences with similarities found from the BLASTP search were aligned to corresponding Msmeg protein sequence (FbpA, FbpB and FbpC).

We conducted a BLASTP search to identify sequences closely resembling the Msmeg FbpA protein and compared it to sequences from Mtb, Ec, Sm, Staph, and Kp. We identified sequences from the other organisms with the highest similarity to the Msmeg FbpA protein sequence. Using Benchling, we aligned these selected sequences to the Msmeg FbpA protein sequence, excluding Bs due to the absence of similar sequences. *Streptococcus respiraculi* was chosen in place of *Streptococcus mutans* (Sm) because Sm was not present in the NCBI data bank. The alignment revealed a 56.81% sequence alignment between Msmeg and Mtb, both being mycobacterial species. This alignment percentage served as a benchmark to pinpoint important sites within the sequence likely involved in similar protein functions. The parts of the Mtb sequence that appeared to be different from the Msmeg FbpA protein sequence may be attributed to differences in protein organization, rather than protein function. Ec, *Streptococcus respiraculi* (in place of Sm), Staph and Kp had alignment pairwise identifies of 12.17%, 17.97%, 19.13% and 14.49% respectively. Through this BLASTP search we determined that there is no significant similarity between the Msmeg FbpA protein sequence and any sequences in Ec, Bs, Sm, Staph and Kp.

We performed a BLASTP search and subsequent sequence alignment of the Msmeg FbpB protein sequence against sequences from Mtb, Ec, Bs, Sm, Staph, and Kp to explore the presence of homologous proteins across different bacterial genera. The search did not yield any similar protein sequences for Bs. Alignment was performed on sequences from Mtb, Ec, *Streptococcus catagoni* (representing Sm), Staph, and Kp, as illustrated in Figure 14b. Pairwise identity percentages were calculated as 70.69%, 13.9%, 17.22%, 22.05%, and 15.11%, respectively. Based on these results, it was concluded that there is not a significant similarity between the FbpB protein in Msmeg and Ec, Bs, Sm, Staph, and Kp.

The FbpC protein sequence alignment search was performed against Mtb, Ec, Bs, *Streptococcus intantis* (in place of Sm), Staph and Kp. The pairwise identities were 72.33%, 14.41%, 8.65%, 17%, 19.31% and 13.83%. Based on these results and the alignment pairings in Figure 14c, we determined that there is no significant similarity between protein FbpC in Msmeg and Ec, Bs, Sm, Staph and Kp.

**Based on these results, we conclude that there are no homologous proteins that have functions similar to those in the Ag85 pathway.** This is in line with literature research on the topic of mycolic acid synthesis in the mycomembrane.[25] This leads us to believe that, unlike with DMN-Tre, it is not the synthesis and incorporation of TMM into TDM in the mycomembrane that is causing 3HC-Tre to label Ec, Bs, Sm, Staph and Kp. Further studies need to be done to determine what is the mechanism of labeling of 3HC-Tre in non-mycobacterial organisms. More discussion on future research can be found in the next chapter.

## Chapter 5: Conclusion and Future Directions

**In this study, we demonstrate that DMN-Tre can be used to selectively label mycobacteria and could be a powerful tool for the rapid diagnosis of TB.** Specifically, our findings highlight the specificity of DMN-Tre for mycobacteria, as evidenced by significantly higher fluorescence FC values of Msmeg compared to Ec, Bs, Sm, Staph and Kp on both the flow cytometer and plate reader. Microscopy results further corroborated the specific DMN-Tre labeling of Msmeg. However, despite its potential, challenges remain concerning the sensitivity of plate readers and the nonspecific labeling observed with 3HC-Tre.

We have determined that 3HC-Tre specificity is limited, as demonstrated through flow cytometry, plate reader and microscopy. Both flow cytometry and plate reader data showed statistically significant fluorescence values of 3HC-Tre labeled cells compared to unlabeled cells for all six organisms. The microscopy showed 3HC-Tre labeling of Msmeg, Ec, Staph and Kp. Bs and Sm do not show 3HC-Tre labeling through microscopy. Further tests are required to determine the reason for the inconsistency between microscopy results and flow cytometry/plate reader results for Bs and Sm.

Although limited by low specificity, 3HC-Tre preprocessed samples may still produce highly sensitive, phenotypic, rapid, low-cost DST solutions. The main advantage of 3HC-Tre is its ability to fluoresce much brighter than DMN-Tre. If further studies are conducted to determine the root cause of the nonspecific labeling, 3HC-Tre or a similar chemical probe could be used as a very helpful TB diagnostic tool.

Both Tre-probes have been shown to only detect live, viable bacteria unlike Ziehl-Neelsen (ZN) smear microscopy and GeneXpert MTB/RIF (Figure S7). $OD_{600}$ alone is not an adequate diagnostic tool because depending on how the cells die they may be counted in the absorbance reading.[26] For this reason colony forming unit (CFU) assays have also been done in the Kamariza lab to verify the $OD_{600}$ measurements are in line with viable cells. The inability to rely on $OD_{600}$ readings for cell viability is a reason why the Tre-probes could be helpful tools for DST.

The study's limitations include the lack of testing with clinical samples and samples containing multiple organisms, as well as the challenges encountered with plate reader sensitivity and nonspecific labeling with 3HC-Tre. These limitations warrant consideration in interpreting the results and planning future research.

**Future Directions**

A trehalose competition assay could provide illuminating information about the metabolic incorporation of the Tre-probes. Here, Tre-probes and varying concentrations of trehalose are introduced to cells to assess if exogenous trehalose affects the metabolism of the probes. This assay, particularly relevant for the nonspecific 3HC-Tre probe, aims to determine if increased trehalose concentrations result in reduced 3HC-Tre labeling, indicating competition for metabolic incorporation. Furthermore, in Ec, Bs, Sm, Staph and Kp, the mechanism of incorporation and/or fluorescence remains unclear. If excess trehalose has no significant impact on labeling, it suggests that 3HC-Tre might be getting stuck between cells, causing elevated fluorescence values. Additionally, experiments using Ebselen to inhibit the Ag85 pathway were conducted in these

organisms but were discontinued due to Ebselen induced cell death of non-mycobacteria, preventing the assessment of Ag85 pathway inhibition on probe labeling.

Additional experiments could investigate whether Tre-probes necessitate a completely hydrophobic environment for fluorescence. It is anticipated that both DMN-Tre and 3HC-Tre require such conditions to fluoresce. If 3HC-Tre does not exhibit this requirement, it could be contributing to the nonspecific labeling demonstrated by the probe.

A future study could focus on microscopy of Msmeg Mcherry and Ec, Bs, Sm, Staph and Kp. Mcherry is shown in the Red Fluorescent Protein (RFP) channel and DMN-Tre labeling appears in GFP and CFP channels. In this test we would be able to validate that the cells showing labeling above autofluorescence of unlabeled cells are the mycobacteria.

Through this thesis we have effectively proven that DMN-Tre specifically labels mycobacteria and 3HC-Tre is not a specific probe. **Our over-arching goal for the Tre- probes is to incorporate them into powerful drug susceptibility tools to provide vital and life-changing diagnostic information to aid in the eradication of TB worldwide.**

## Supplemental Information

A

$$y = 0.1114 + \frac{41.99}{1 + 10^{(1.526x(2.457-x))}}$$

$R^2 = 0.9452$

B

$$y = 0.1048 + \frac{1.219}{1 + 10^{(1.847x(0.9597-x))}}$$

$R^2 = 0.8564$

C

$$y = 0.1096 + \frac{2.903}{1 + 10^{(1.601x(0.3957-x))}}$$

$R^2 = 0.7833$

D

$$y = 0.1844 + \frac{2.600}{1 + 10^{(0.5275x(1.574-x))}}$$

$R^2 = 0.9791$

E

$$y = 0.09618 + \frac{1.532}{1 + 10^{(2.689x(0.5778-x))}}$$

$R^2 = 0.9740$

F

$$y = 0.1086 + \frac{0.6000}{1 + 10^{(2.472x(0.8295-x))}}$$

$R^2 = 0.9940$

**Figure S1. Growth curve equations from nonlinear regression analysis generated on GraphPad Prism. (A)** Msmeg **(B)** Ec **(C)** Bs **(D)** Sm **(E)** Staph **(F)** Kp. Nonlinear regression analysis completed on graphs from Figure 3.

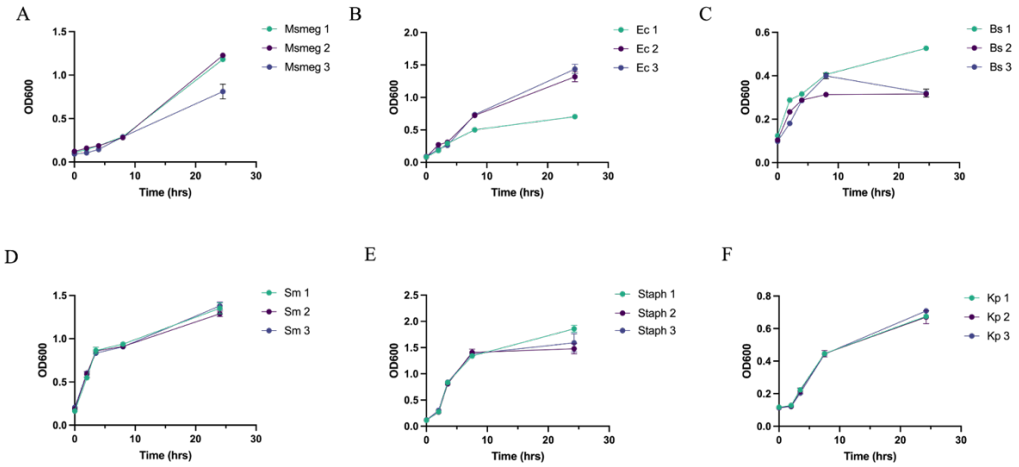


**Figure S2. Growth curves demonstrate exponential growth of all six organisms. (A)** Msmeg, **(B)** Ec, **(C)** Bs, **(D)** Sm, **(E)** Staph and **(F)** Kp cells were grown in 7H9, LB, brain heart infusion broth, tryptic soy broth and Difco nutrient broth respectively. Cultures were diluted to an $OD_{600}$ of 0.1 and measurements were taken periodically for about 25 hours to determine growth rates. Each graph is representative of three biological replicates.

A

$y = 0.1064e^{0.124x}$

$R^2 = 0.9997$

B

$y = 0.1456e^{0.1853x}$

$R^2 = 0.9962$

C

$y = 0.2089e^{0.0747x}$

$R^2 = 0.9639$

D

$y = 0.5584e^{0.0684x}$

$R^2 = 0.7037$

E

$y = 0.2266e^{0.2551x}$

$R^2 = 0.8619$

F

$y = 0.087e^{0.2222x}$

$R^2 = 0.9848$

**Figure S3. Exponential equations and $R^2$ from exponential trendline demonstrate exponential growth rate. (A)** Msmeg **(B)** Ec **(C)** Bs **(D)** Sm **(E)** Staph **(F)** Kp. Excel exponential trendline run on average $OD_{600}$ values for T = 2, 4, 8 for Msmeg, Ec, Bs, Sm and T = 2, 3.5, 7.5 for Staph and Kp (data from Figure 3).

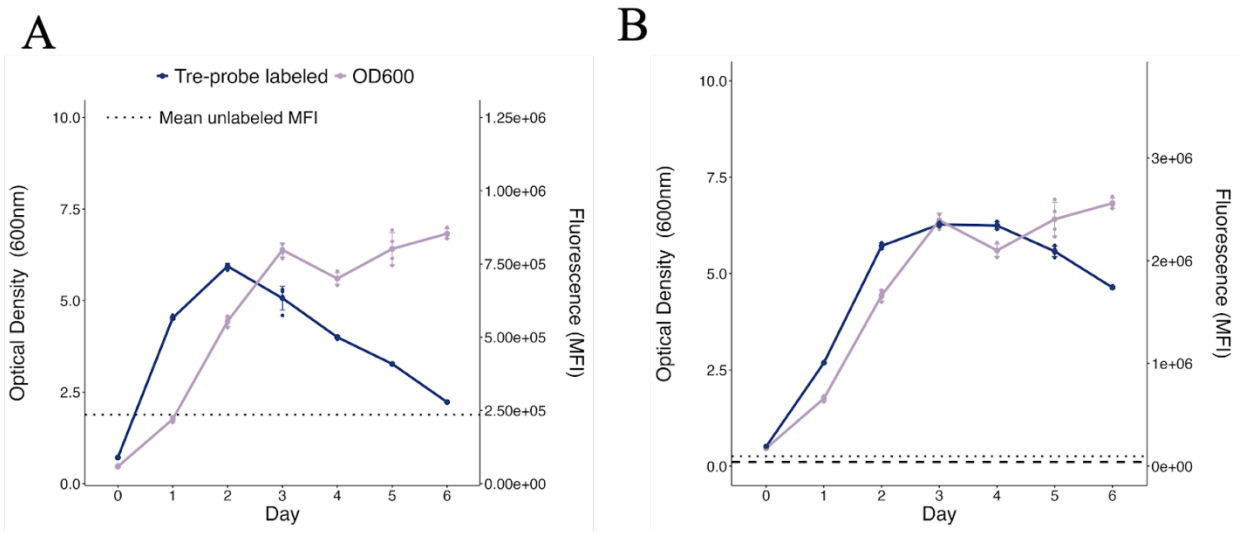


**Figure S4. Fluorescence intensity decreases at stationary phase, even as $OD_{600}$ increases. (A)** 100 µM DMN-Tre labeled Msmeg samples. **(B)** 10 µM 3HC-Tre labeled Msmeg samples. Total sample volume: 800 µL. After Tre-probe treatment all samples incubated for 30 mins and then washed out twice with DPBS. Fluorescence and $OD_{600}$ measurements collected on plate reader. MFI is Mean Fluorescence Intensity. Data collected by Amelia Rodolf.

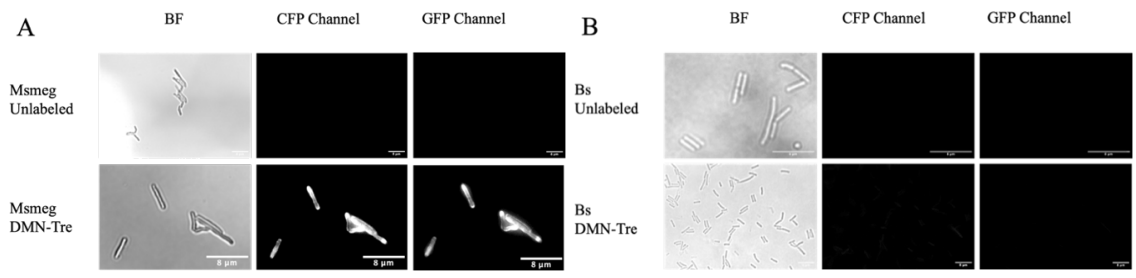


**Figure S5. DMN-Tre labeled Msmeg cells are brighter than DMN-Tre labeled Bs cells.** All cultures diluted to $OD_{600}$: 0.5 treated with or without 100 µM DMN-Tre depending on the sample and incubated for 30 minutes. **(A)** Msmeg images taken with 60x objective. **(B)** Unlabeled images taken with 160x objective and DMN-Tre labeled images taken with 60x objective. All CFP channel TIF microscopy images were edited on FIJI to display brightness/contrast minimum displayed value of 6,200 and maximum displayed value of 38,000. All GFP channel images have a minimum displayed value of 5,700 and maximum displayed value of 34,000. Scale bar: 8 µm.

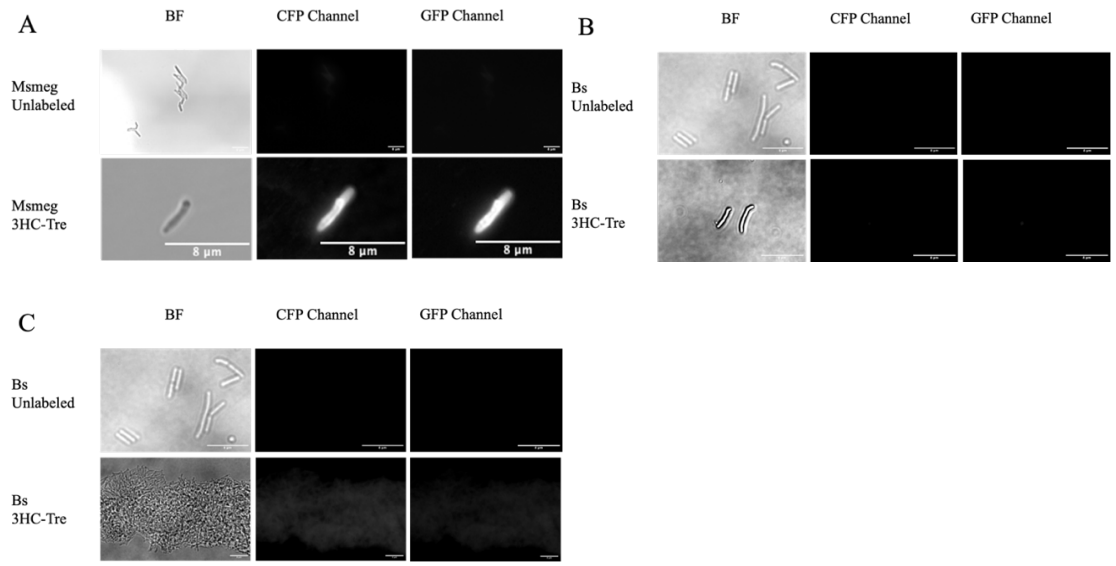


**Figure S6. 3HC-Tre labeled Msmeg cells are brighter than 3HC-Tre labeled Bs cells.** All cultures diluted to $OD_{600}$: 0.5 treated with or without 10 µM 3HC-Tre depending on the sample and incubated for 30 minutes. **(A)** Msmeg images taken with 60x objective. **(B)** and **(C)** Bs images taken with 160x objective. All CFP channel TIF microscopy images were edited on FIJI to display brightness/contrast minimum displayed value of 6,200 and maximum displayed value of 38,000. All GFP channel images have a minimum displayed value of 5,700 and maximum displayed value of 34,000. Scale bar: 8 µm.

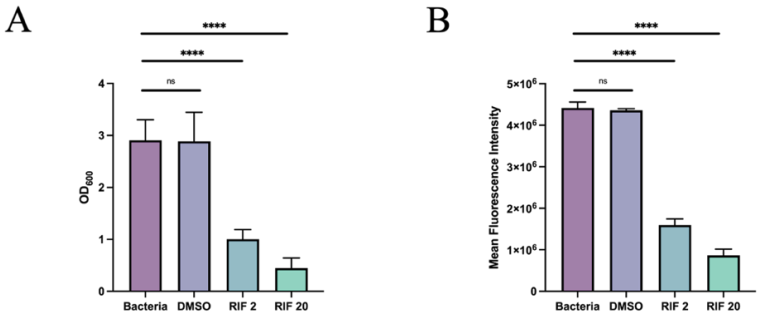


**Figure S7. 3HC-Tre fluorescence output on plate reader shows similar trend to $OD_{600}$ Readings. (A)** and **(B)** All samples grown to an $OD_{600}$ of 0.5. "Bacteria" samples were not treated with drug. "DMSO" samples were treated with 20 µg/ml of dimethyl sulfoxide (DMSO). "RIF 2" samples were treated with 2 µg/ml of rifampicin dissolved in DMSO. "RIF 20" samples were treated with 20 µg/ml of rifampicin dissolved in DMSO. All samples were incubated for 24 hours. (**B)** After 24 hour incubation samples treated with 10 µM 3HC-Tre for 30 minutes and washed 2 times with DPBS. All graphs are representative of three biological replicates. Data collected by Lilith Schwartz, Adriann Brodeth and Cara Susilo.

**Bibliography**


(1) *Global Tuberculosis Report s*. https://www.who.int/teams/global-tuberculosis-programme/tb-reports (accessed 2024-05-31).

(2) Heemskerk, D.; Caws, M.; Marais, B.; Farrar, J. Diagnosis. In *Tuberculosis in Adults and Children*; Springer, 2015.

(3) Singh, S.; Dey, B.; Sachdeva, K.; Kabra, S.; Chopra, K.; Chaudhary, V. K.; Sharma, P.; Katoch, V. Challenges in Tuberculosis Diagnosis and Management: Recommendations of the Expert Panel. *J. Lab. Physicians* **2015**, *7* (1), 1–3. https://doi.org/10.4103/0974-2727.154778.

(4) *Technical manual for drug susceptibility testing of medicines used in the treatment of tuberculosis*. https://www.who.int/publications-detail-redirect/9789241514842 (accessed 2024-06-01).

(5) Shaozae, C. K.; Das, D.; Kumar, M. Diagnosis of Tuberculosis in Low-Resource Settings: Overcoming Challenges Within Laboratory Practice. *Eur. Med. J.* **2023**. https://doi.org/10.33590/emj/10302558.

(6) Wong, C.; Ha, N. P.; Pawlowski, M. E.; Graviss, E. A.; Tkaczyk, T. S. Differentiating between Live and Dead Mycobacterium Smegmatis Using Autofluorescence. *Tuberc. Edinb. Scotl.* **2016**, *101 Suppl*, S119–S123. https://doi.org/10.1016/j.tube.2016.09.010.

(7) Kamariza, M.; Shieh, P.; Ealand, C. S.; Peters, J. S.; Chu, B.; Rodriguez-Rivera, F. P.; Babu Sait, M. R.; Treuren, W. V.; Martinson, N.; Kalscheuer, R.; Kana, B. D.; Bertozzi, C. R. Rapid Detection of Mycobacterium Tuberculosis in Sputum with a Solvatochromic Trehalose Probe. *Sci. Transl. Med.* **2018**, *10* (430), eaam6310. https://doi.org/10.1126/scitranslmed.aam6310.

(8) Banahene, N.; Swarts, B. M. Metabolic Labeling of Live Mycobacteria with Trehalose-Based Probes. In *Mycobacteria Protocols*; Parish, T., Kumar, A., Eds.; Springer US: New York, NY, 2021; pp 385–398. https://doi.org/10.1007/978-1-0716-1460-0_18.

(9) Backus, K. M.; Dolan, M. A.; Barry, C. S.; Joe, M.; McPhie, P.; Boshoff, H. I. M.; Lowary, T. L.; Davis, B. G.; Barry, C. E. The Three Mycobacterium Tuberculosis Antigen 85 Isoforms Have Unique Substrates and Activities Determined by Non-Active Site Regions. *J. Biol. Chem.* **2014**, *289* (36), 25041–25053. https://doi.org/10.1074/jbc.M114.581579.

(10) Boos, W.; Ehmann, U.; Forkl, H.; Klein, W.; Rimmele, M.; Postma, P. Trehalose Transport and Metabolism in Escherichia Coli. *J. Bacteriol.* **1990**, *172* (6), 3450–3461.

(11) Kamariza, M.; Keyser, S. G. L.; Utz, A.; Knapp, B. D.; Ealand, C.; Ahn, G.; Cambier, C. J.; Chen, T.; Kana, B.; Huang, K. C.; Bertozzi, C. R. Toward Point-of-Care Detection of Mycobacterium Tuberculosis: A Brighter Solvatochromic Probe Detects Mycobacteria within Minutes. *JACS Au* **2021**, *1* (9), 1368–1379. https://doi.org/10.1021/jacsau.1c00173.

(12) Boldi, M.-O.; Denis-Lessard, J.; Neziri, R.; Brouillet, R.; von-Garnier, C.; Chavez, V.; Mazza-Stalder, J.; Jaton, K.; Greub, G.; Opota, O. Performance of Microbiological Tests for Tuberculosis Diagnostic According to the Type of Respiratory Specimen: A 10-Year Retrospective Study. *Front. Cell. Infect. Microbiol.* **2023**, *13*, 1131241. https://doi.org/10.3389/fcimb.2023.1131241.

(13) Caulfield, A. J.; Wengenack, N. L. Diagnosis of Active Tuberculosis Disease: From Microscopy to Molecular Techniques. *J. Clin. Tuberc. Mycobact. Dis.* **2016**, *4*, 33–43. https://doi.org/10.1016/j.jctube.2016.05.005.

(14) Raghubanshi, B. R.; Karki, B. M. S. Bacteriology of Sputum Samples: A Descriptive Cross-Sectional Study in a Tertiary Care Hospital. *JNMA J. Nepal Med. Assoc.* **2020**, *58* (221), 24–28. https://doi.org/10.31729/jnma.4807.

(15) Mansoor, S.; Qadir, S.; Javed, S.; Jehan, F. S.; Kundi, M. Antimicrobial Susceptibility of Organisms Isolated from Sputum Culture of Karachi, Pakistan. *Pak. J. Pharm. Sci.* **2017**, *30* (6), 2247–2252.

(16) Regmi, R. S.; Khadka, S.; Sapkota, S.; Adhikari, S.; Dhakal, K. K.; Dhakal, B.; Lamsal, B.; Kafle, S. C. Bacterial Etiology of Sputum from Tuberculosis Suspected Patients and Antibiogram of the Isolates. *BMC Res. Notes* **2020**, *13*, 520. https://doi.org/10.1186/s13104-020-05369-8.

(17) Ngekeng, S.; Pokam, B. T.; Meriki, H. D.; Njunda, A. L.; Assob, J. C. N.; Ane-Anyangwe, I. High Prevalence of Bacterial Pathogens in Sputum of Tuberculosis Suspected Patients in Buea. *Microbiol. Res. J. Int.* **2016**, 1–8. https://doi.org/10.9734/BMRJ/2016/22426.

(18) *Shop Microplate Readers For Sale, New and Used Prices | LabX.com*. https://www.labx.com/categories/microplate-readers (accessed 2024-06-01).

(19) Team, C. *Unlocking Insights: Flow Cytometer Price Guide*. Merkel Technologies Ltd. https://merkel.co.il/flow-cytometer-price-guide/ (accessed 2024-06-01).

(20) *Gallery*. https://app.biorender.com/ (accessed 2024-05-31).

(21) *9: Microbial Growth*. Biology LibreTexts. https://bio.libretexts.org/Bookshelves/Microbiology/Microbiology_(Bruslind)/09%3A_Microbial_Growth (accessed 2024-06-09).

(22) Bradner, L.; Robbe-Austerman, S.; Beitz, D. C.; Stabel, J. R. Chemical Decontamination with N-Acetyl-l-Cysteine–Sodium Hydroxide Improves Recovery of Viable Mycobacterium Avium Subsp. Paratuberculosis Organisms from Cultured Milk. *J. Clin. Microbiol.* **2013**, *51* (7), 2139–2146. https://doi.org/10.1128/JCM.00508-13.

(23) Yang, L.; Zhou, Y.; Zhu, S.; Huang, T.; Wu, L.; Yan, X. Detection and Quantification of Bacterial Autofluorescence at the Single-Cell Level by a Laboratory-Built High-Sensitivity Flow Cytometer. *Anal. Chem.* **2012**, *84* (3), 1526–1532. https://doi.org/10.1021/ac2031332.

(24) *Flavin - an overview | ScienceDirect Topics*. https://www.sciencedirect.com/topics/biochemistry-genetics-and-molecular-biology/flavin (accessed 2024-06-08).

(25) North, E. J.; Jackson, M.; Lee, R. E. New Approaches to Target the Mycolic Acid Biosynthesis Pathway for the Development of Tuberculosis Therapeutics. *Curr. Pharm. Des.* **2014**, *20* (27), 4357–4378.

(26) Kesisoglou, I.; Tam, V. H.; Tomaras, A. P.; Nikolaou, M. Discerning in Vitro Pharmacodynamics from OD Measurements: A Model-Based Approach. *Comput. Chem. Eng.* **2022**, *158*, 107617. https://doi.org/10.1016/j.compchemeng.2021.107617.